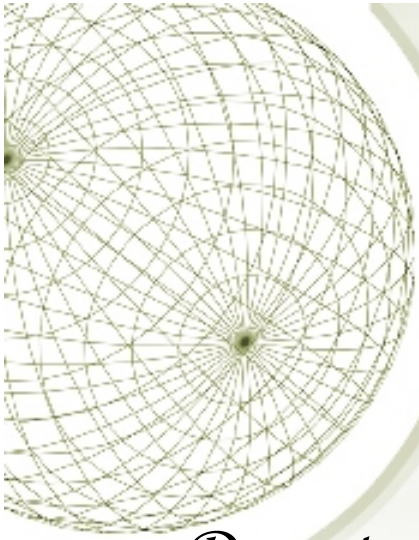

Polarized Light in Nature

George W. Kattawar

Department of Physics and Institute for Quantum Science and Engineering

Texas A&M University

Research Colleagues:

Meng Gao, Ping Yang,and Yu You

TEXAS A&M UNIVERSITY

Electromagnetic waves were first postulated by James Clerk Maxwell in 1862 and subsequently confirmed by Heinrich Hertz in 1887.

In 1864, Maxwell wrote "A dynamical theory of the electromagnetic field", where he first proposed that light was in fact undulations in the same medium that is the cause of electric and magnetic phenomena.

Maxwell derived a wave form of the electric and magnetic equations, revealing the wave-like nature of electric and magnetic fields, and their symmetry. His work in producing a unified model of electromagnetism is considered to be one of the greatest advances in physics.

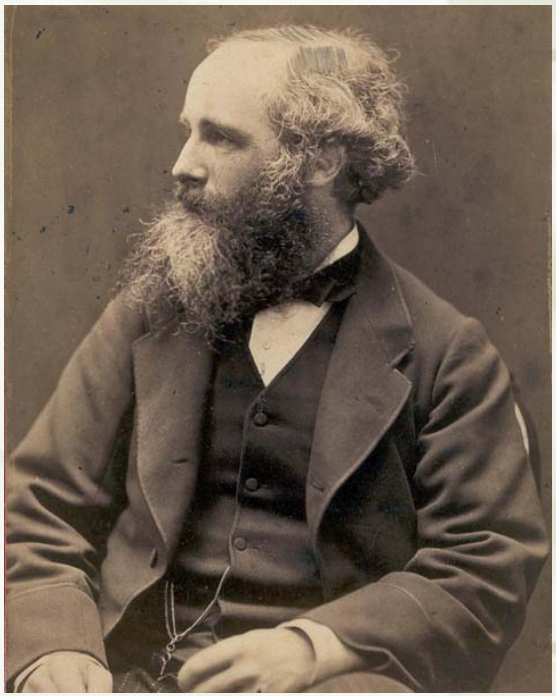

And God said

$$\partial \mathbf{E}/\partial t = c\nabla \times \mathbf{B} - 4\pi \mathbf{j}$$

$$\partial \mathbf{B}/\partial t = -c\nabla \times \mathbf{E}$$

$$\nabla \cdot \mathbf{E} = 4\pi\rho$$

$$\nabla \cdot \mathbf{B} = 0$$

And then there was light

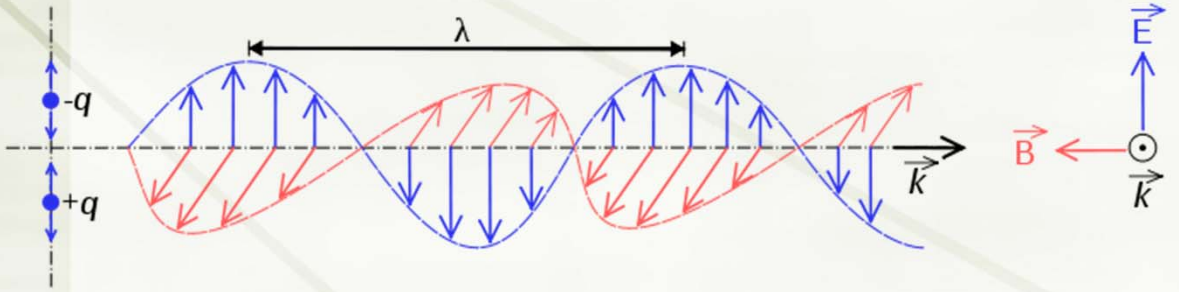

What is refractive index?

The refractive index n (or index of refraction) of a medium is a measure of how much the velocity of a wave is reduced inside that medium.

$$n = \frac{c}{v_P} = \frac{\lambda_{vacuum}}{\lambda_{medium}}$$

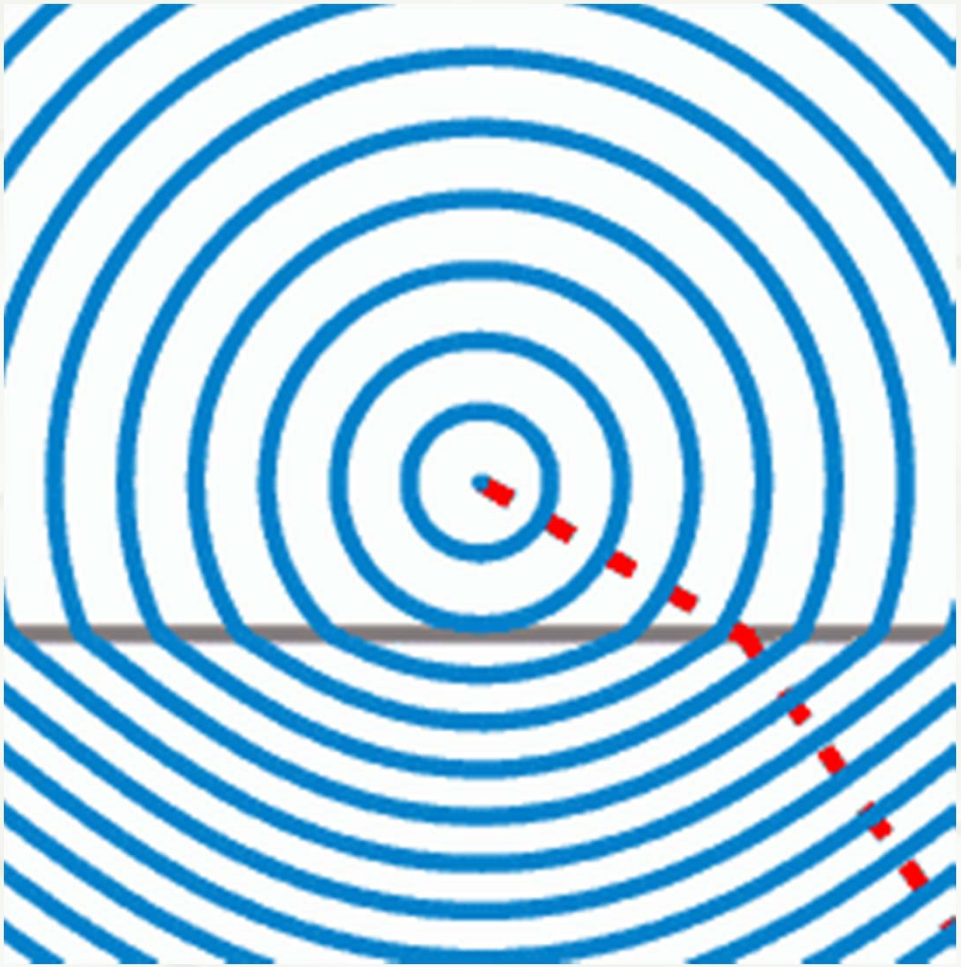

Wavefronts from a point source in the context of Snell's law. The region below the gray line has a higher index of refraction and proportionally lower wave velocity than the region above it.

Component decomposition of linear Polarization

Linearly Polarized Light

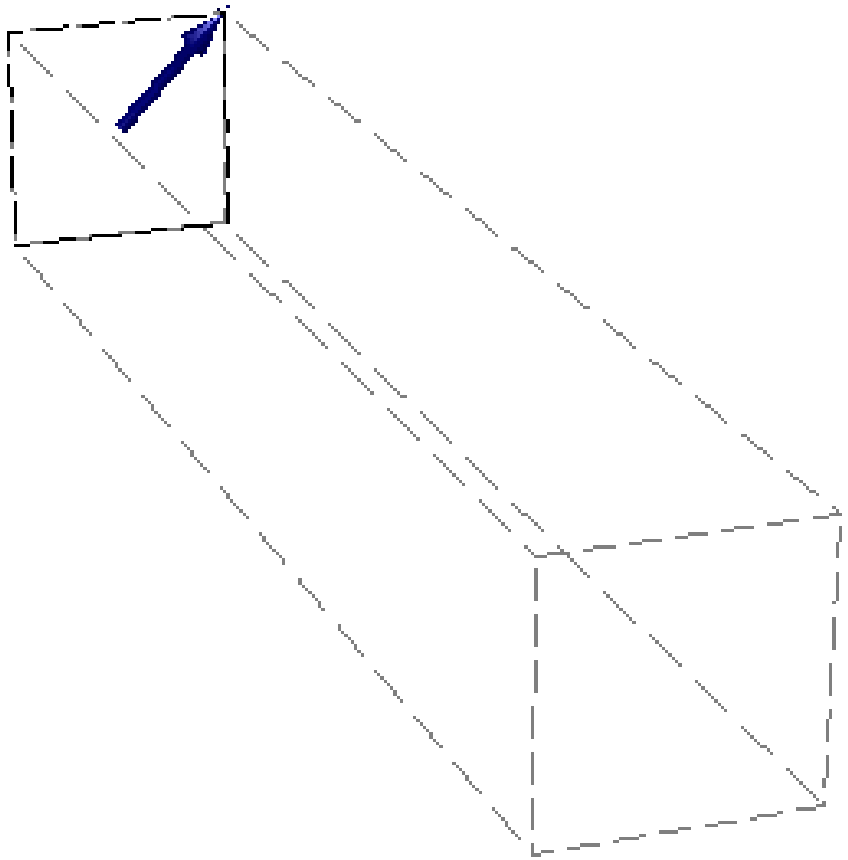

Component decomposition of circular Polarization

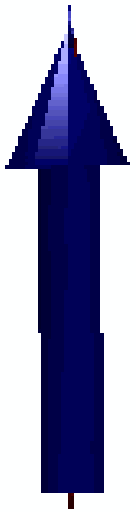

Circularly Polarized Light

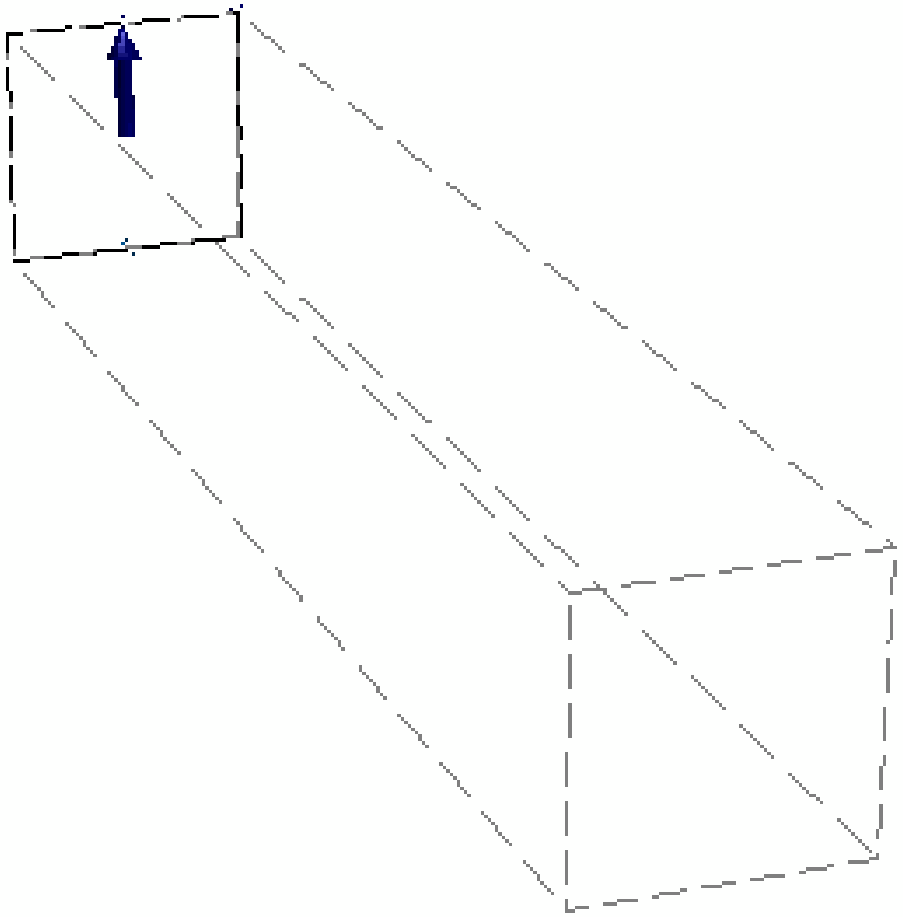

Linear Polarizer

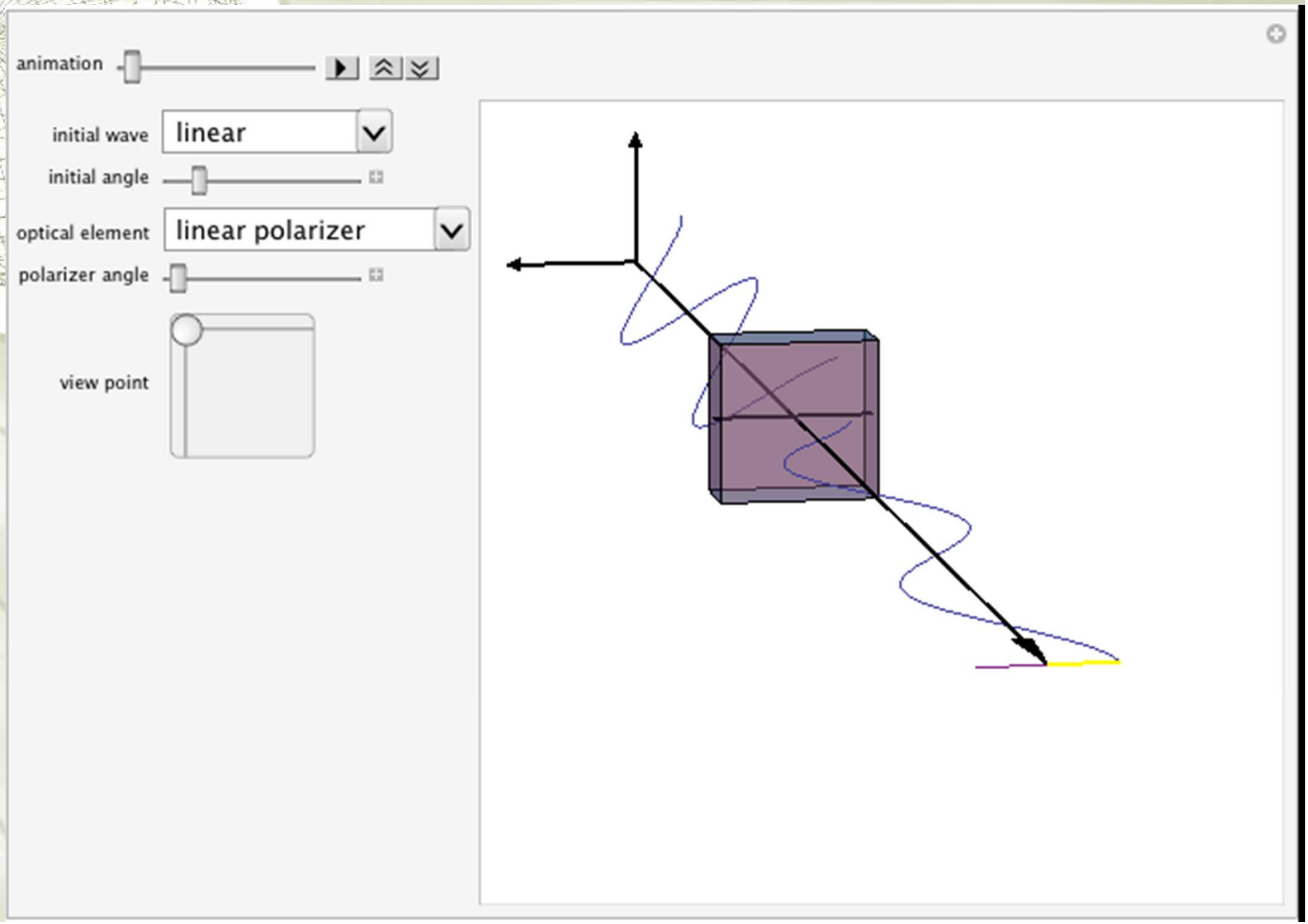

Quarter Wave Plate

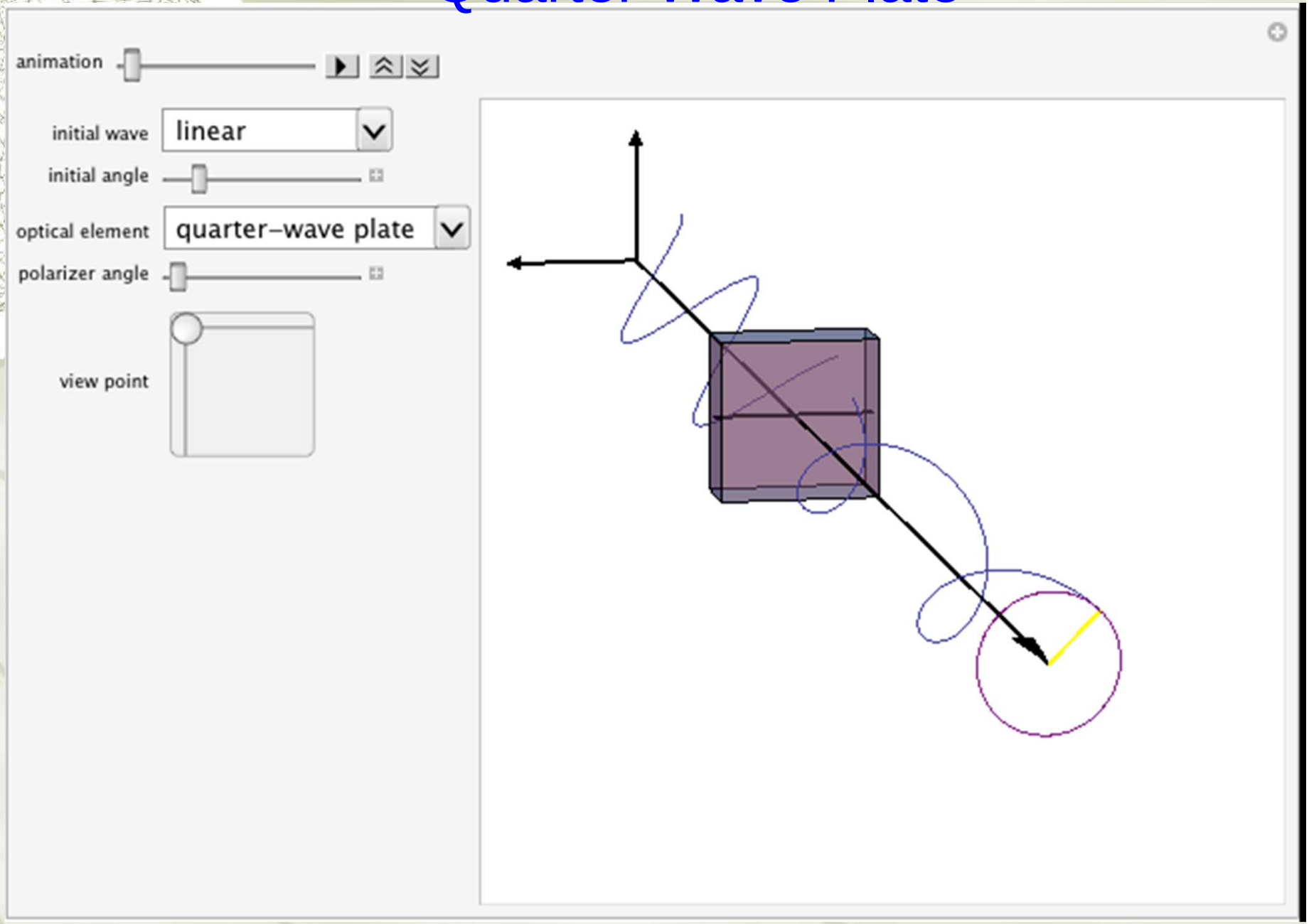

Scattering Geometry

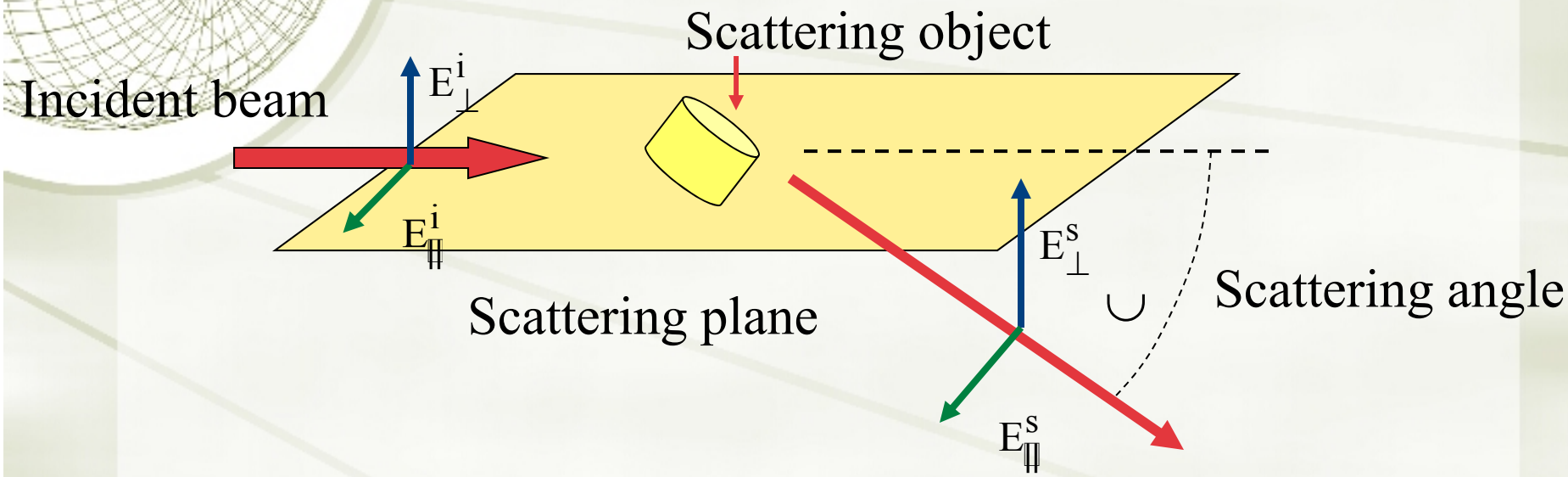

Stokes vector-Mueller matrix formulation

The electric field can be resolved into components. E_l and E_r are complex oscillatory functions.

$$\vec{E} = E_l \hat{l} + E_r \hat{r}$$

The four component Stokes vector can now be defined.

They are all real numbers and satisfy the relation

$$I^2 = Q^2 + U^2 + V^2$$

$$I = I_l + I_r$$

$$Q = I_l - I_r$$

$$U = I_{45^0} - I_{135^0}$$

$$V = I_R - I_L$$

The Mueller matrix relates the incident and scattered Stokes vectors

$$\begin{pmatrix} I^s \\ Q^s \\ U^s \\ V^s \end{pmatrix} = \begin{pmatrix} M_{11} & M_{12} & M_{13} & M_{14} \\ M_{21} & M_{22} & M_{23} & M_{24} \\ M_{31} & M_{32} & M_{33} & M_{34} \\ M_{41} & M_{42} & M_{43} & M_{44} \end{pmatrix} \begin{pmatrix} I^i \\ Q^i \\ U^i \\ V^i \end{pmatrix}$$

Homogenous Cylinder Mueller Image

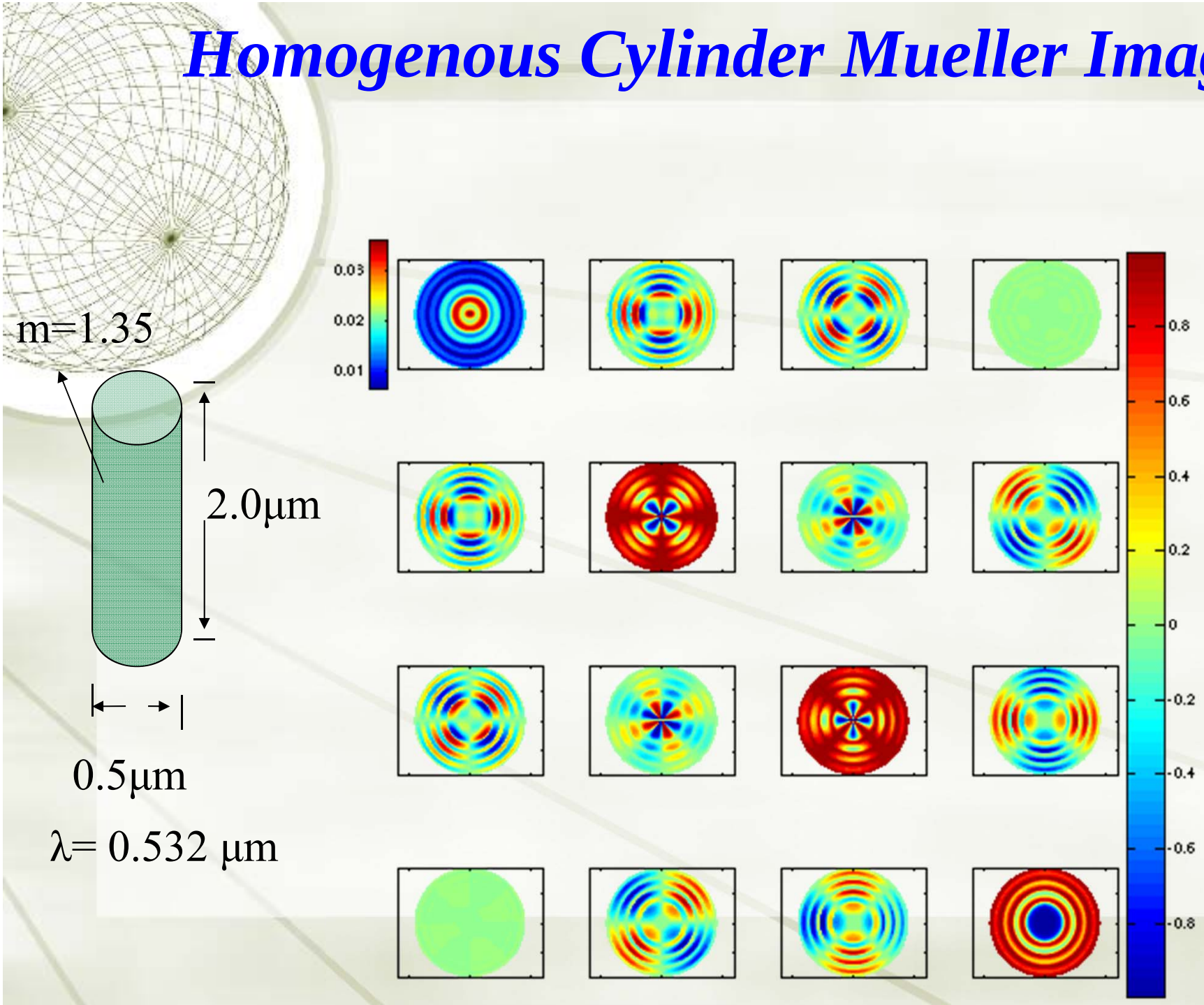

Stokes vector and polarization parameters

I is the radiance (this is what the human eye sees)

Q is the amount of radiation that is polarized in the $0/90^0$ orientation

U is the amount of radiation polarized in the $+/-45^0$ orientation

V is the amount of radiation that is right or left circularly polarized

DOP= Degree of polarization= $\sqrt{Q^2 + U^2 + V^2} / I$

DOLP = Degree of linear polarization = $\sqrt{Q^2 + U^2} / I$

DOCP = Degree of circular polarization = $|V|/I$

Orientation of plane of polarization = $\chi = \tan^{-1}(U/Q)/2$

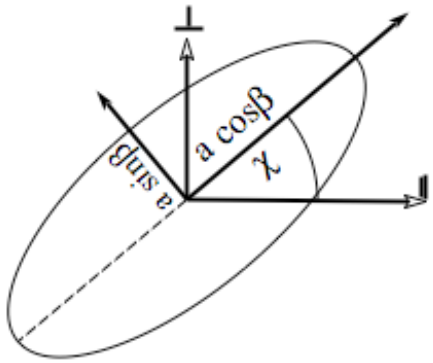

Ellipticity= Ratio of semiminor to semimajor axis of polarization ellipse = b/a

$=\tan[(\sin^{-1}(V/I))/2]$

Nissan car viewed in mid-wave infrared

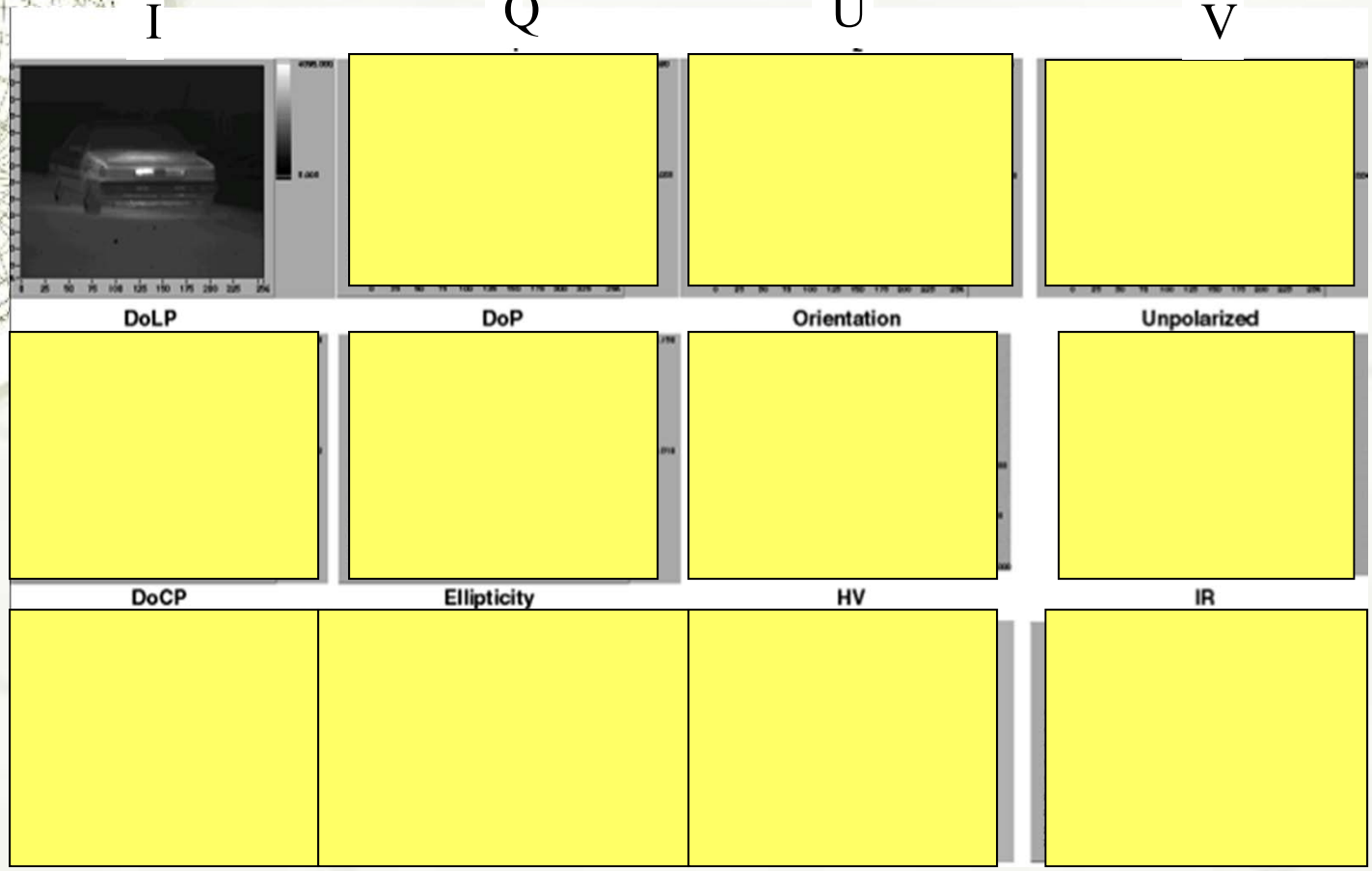

This data was collected using an Amber MWIR InSb imaging array 256x256. The polarization optics consisted of a rotating quarter wave plate and a linear polarizer. Images were taken at eight different positions of the quarter wave plate (22.5 degree increments) over 180 degrees. The data was reduced to the full Stokes vector using a Fourier transform data reduction technique.

Haidinger's Brush

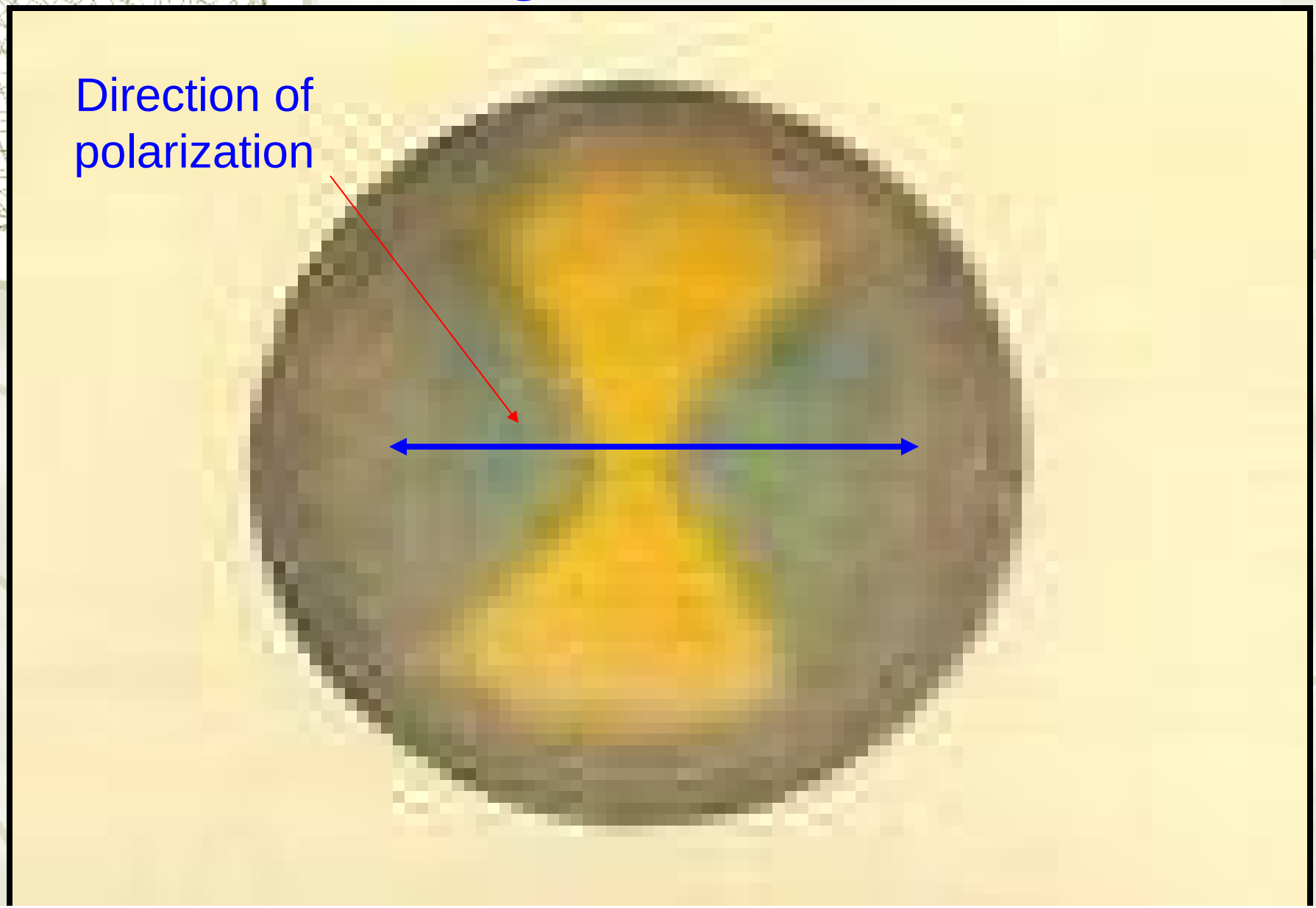

Snell's Law

$$n_1 \sin\theta_1 = n_2 \sin\theta_2$$

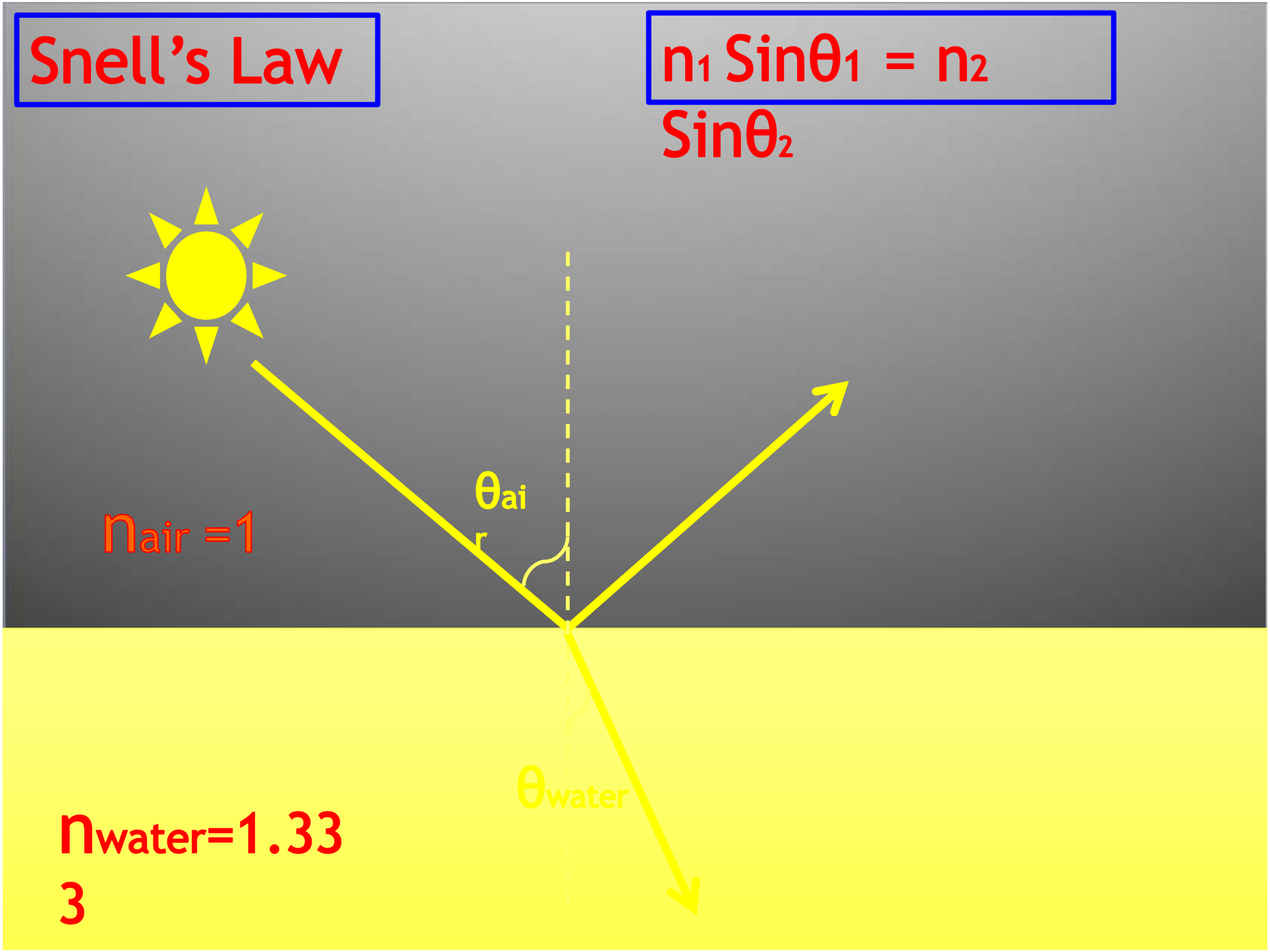

Snell's Window

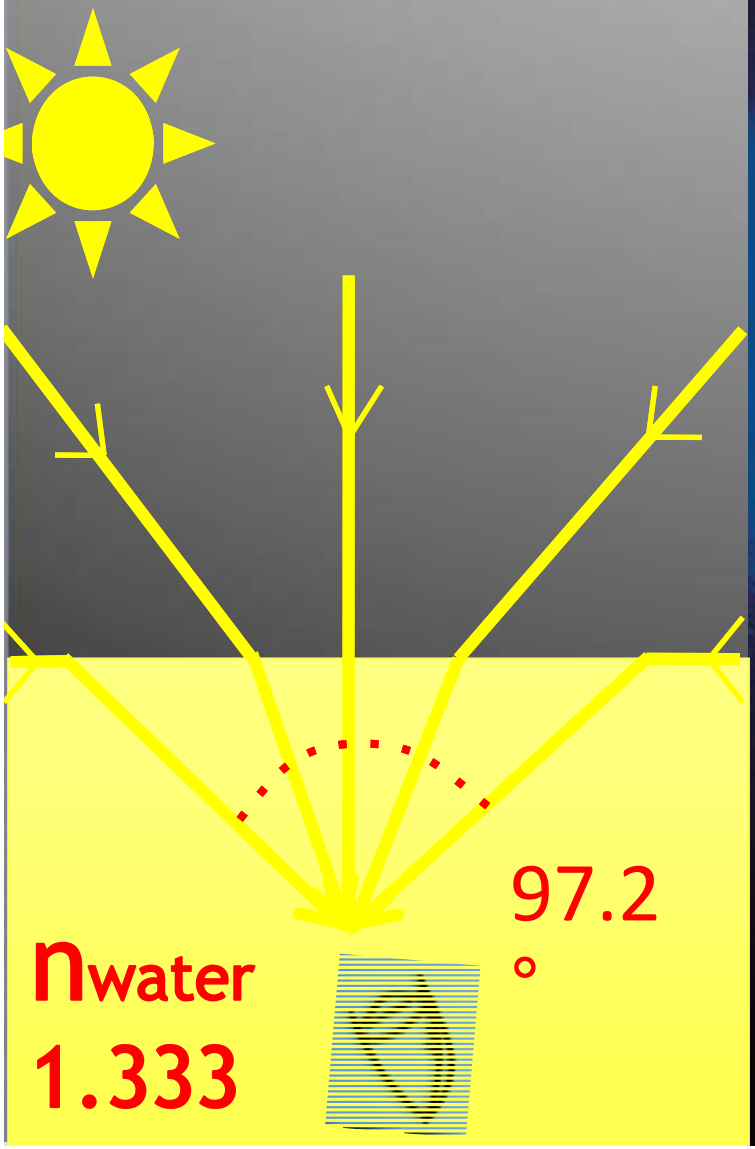

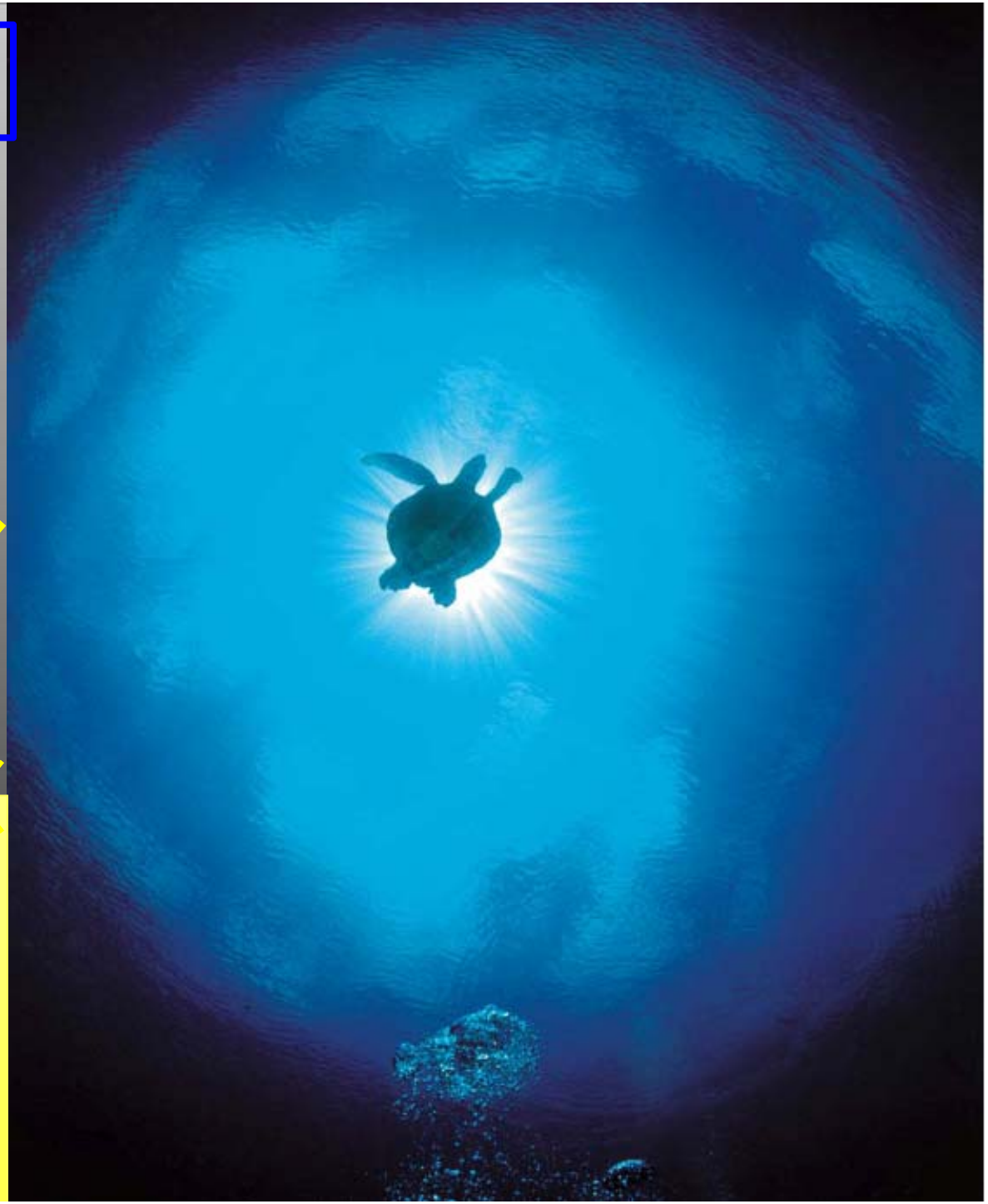

Brewster's Angle θ_B

$\tan \theta_B = n$

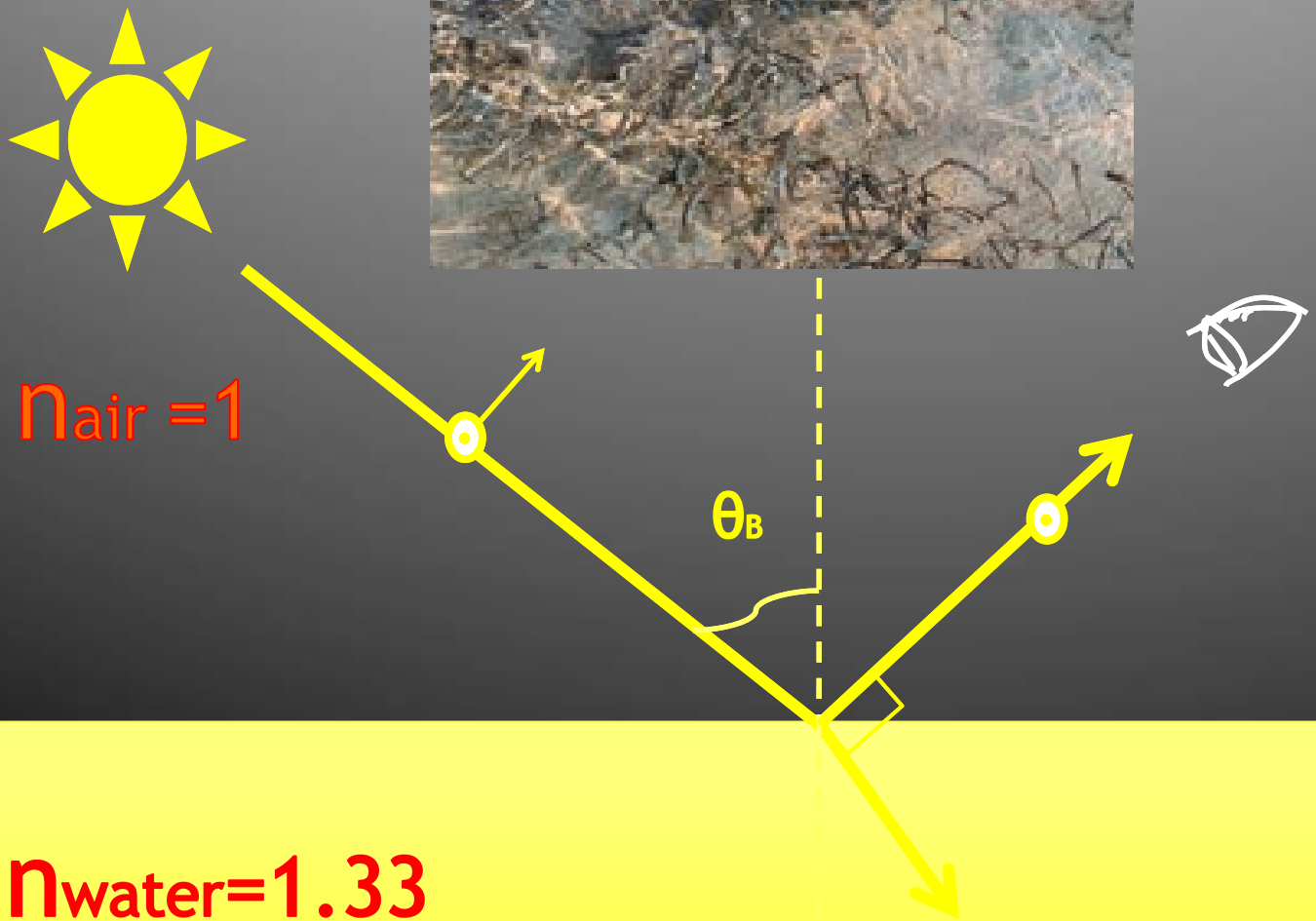

Brewster's Angle θ_B

$\tan \theta_B = n$

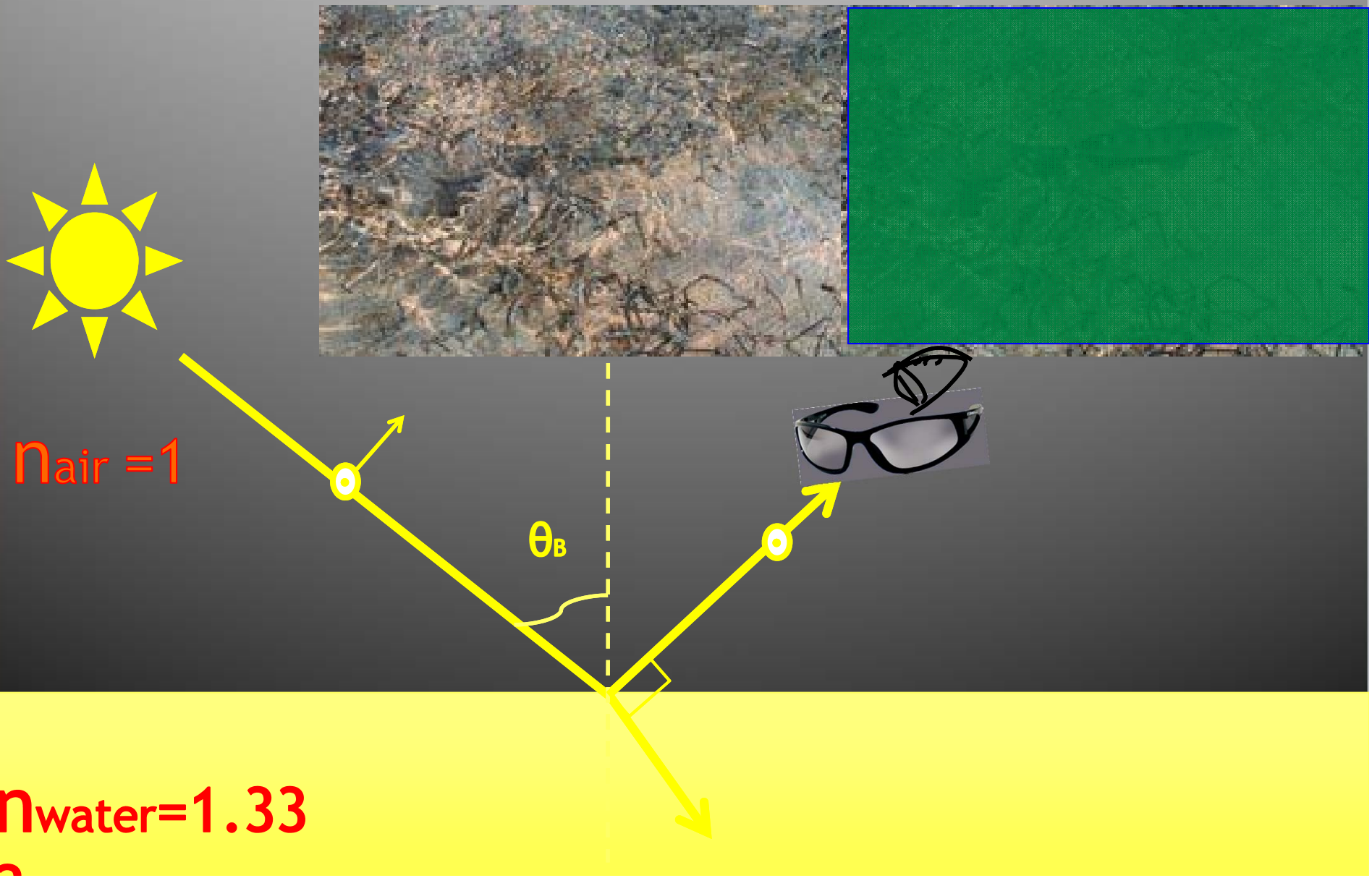

Contrast enhancement using polarization

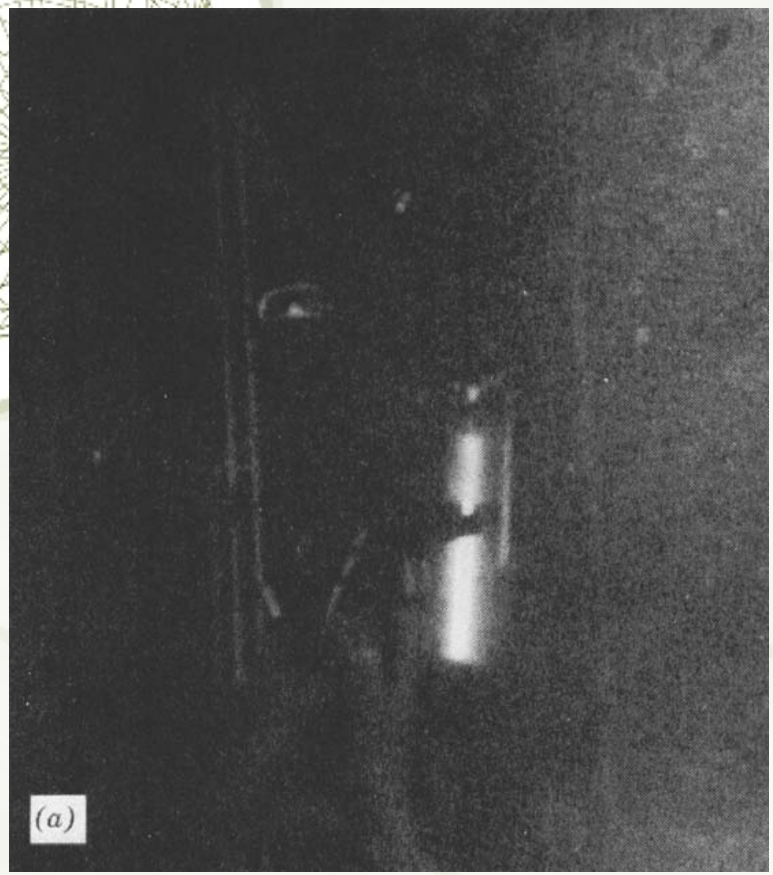

Photo taken with a flash lamp and no polarization optics

Photo taken with circular polarized light for illumination and a circular analyzer for viewing

The single-scatter reduced Mueller matrix for ocean water is basically Rayleigh scattering:

$$\tilde{M}(180^0) = \begin{bmatrix} 1 & 0 & 0 & 0 \\ 0 & 1 & 0 & 0 \\ 0 & 0 & -1 & 0 \\ 0 & 0 & 0 & -1 \end{bmatrix}$$

$$\begin{bmatrix} 1 & 0 & 0 & 0 \\ 0 & 1 & 0 & 0 \\ 0 & 0 & -1 & 0 \\ 0 & 0 & 0 & -1 \end{bmatrix} \begin{bmatrix} 1 \\ 0 \\ 0 \\ 1 \end{bmatrix} = \begin{bmatrix} 1 \\ 0 \\ 0 \\ -1 \end{bmatrix}$$

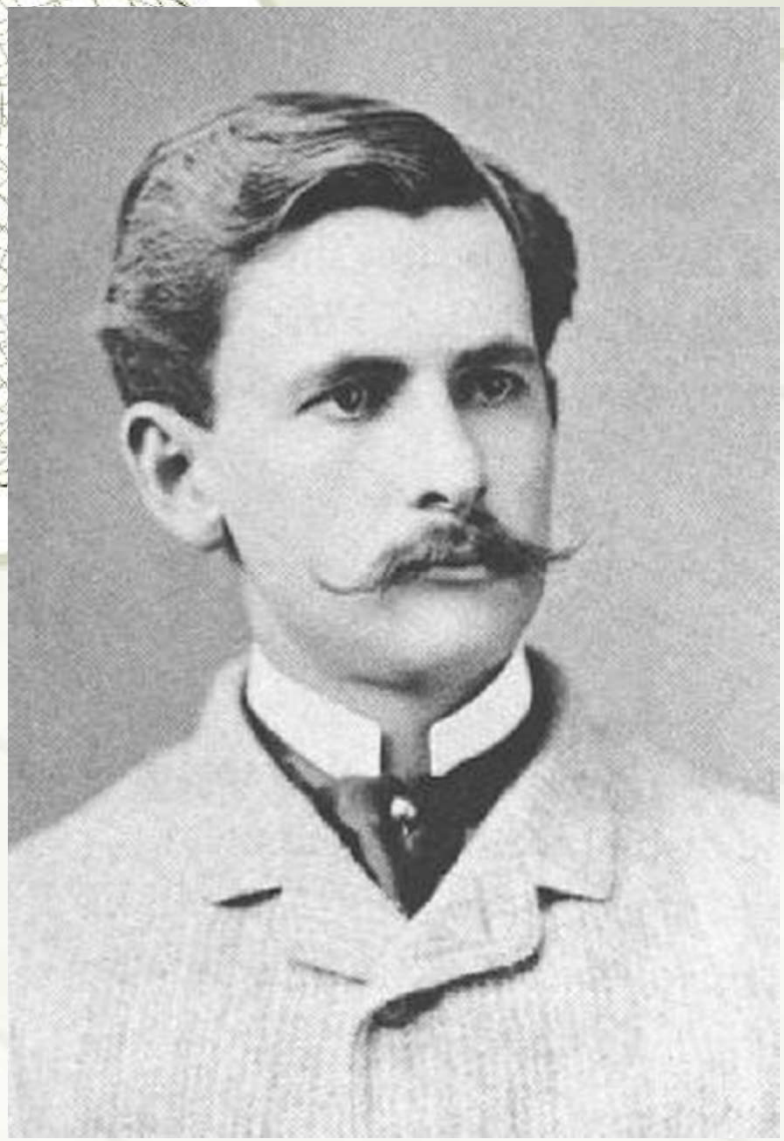

Albert Abraham Michelson

"The aesthetic side of the subject is by no means the least attractive to me. I hope the day is near when a Ruskin will be found equal to the description of the beauties of coloring, the exquisite gradations of light and shade, and the intricate wonders of symmetrical forms and combinations which are encountered everywhere."

"On Metallic Colouring in Birds and Insects", Philos. Mag. 21, 554-567, (1911)

Plusiotis woodi

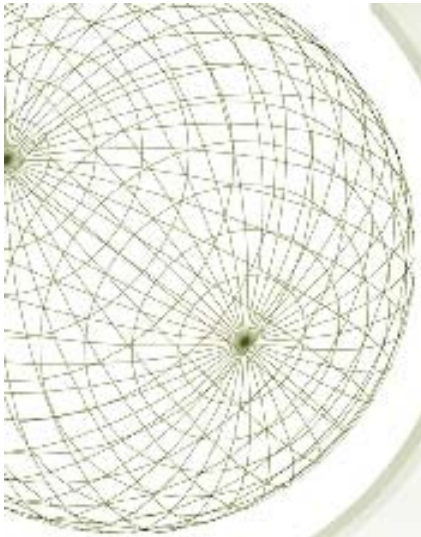

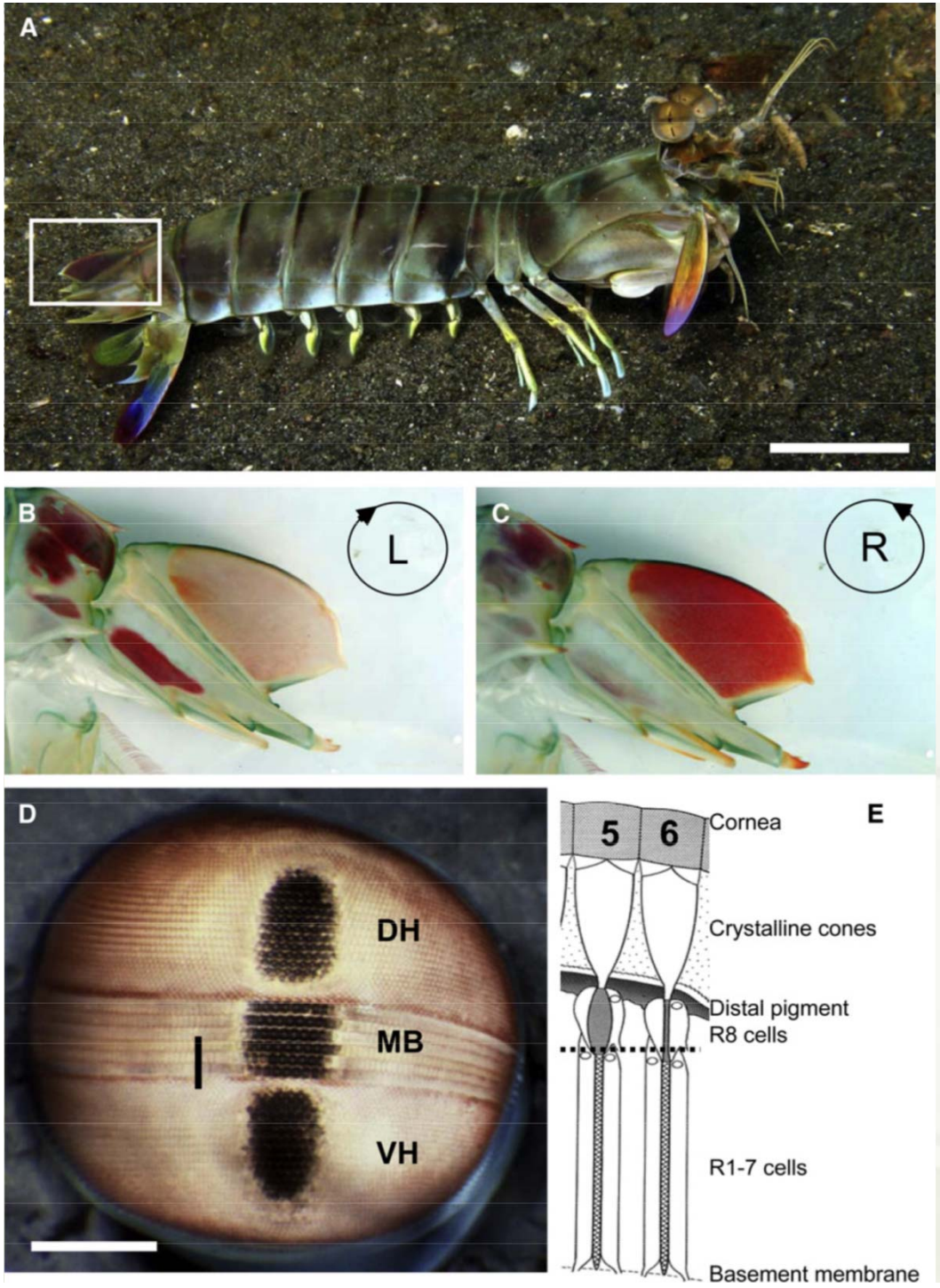

Figure 1. Circular Polarizing Signals and General Eye Anatomy in Stomatopods

(A) The stomatopod crustacean Odontodactylus cultrifer (male). The scale bar represents 1 cm. (Photograph by Chrissy Huffard.)

(B) Detail of telson keel (inset in [A]) photographed through a left-handed circular polarizing filter.

(C) As (B) except photographed through a right-handed circular polarizing filter. Note the striking contrast difference compared to (B).

(D) The eye of Odontodactylus scyllarus, a close relative of O. cultrifer, seen from the front. The vertical line is section direction and extent in (E).
The following abbreviations are used: midband (MB), dorsal hemisphere (DH), and ventral hemisphere (VH). The scale bar represents 800 mm.
(E) Diagrammatic representation of a sagittal section (line in [D]) of rows five and six of the midband of the eye of a generalized gonodactyloid stomatopod.

Chiou et al., Current Biology, 18, 429-434 (2008)

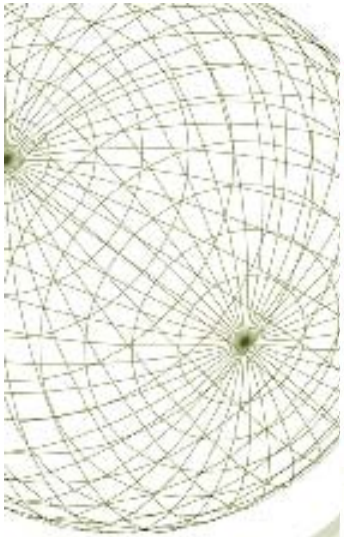

A

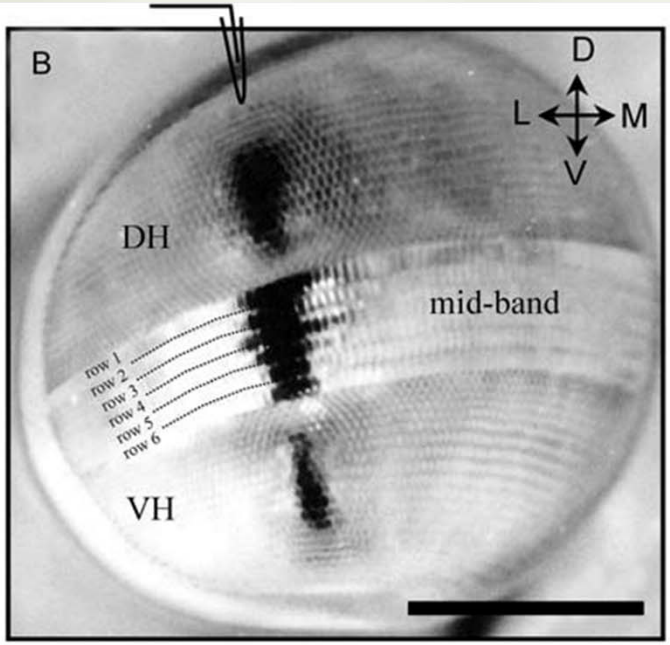
B
D
L
M
V
DH
mid-band
row 1
row 2
row 3
row 4
row 5
row 6
VH

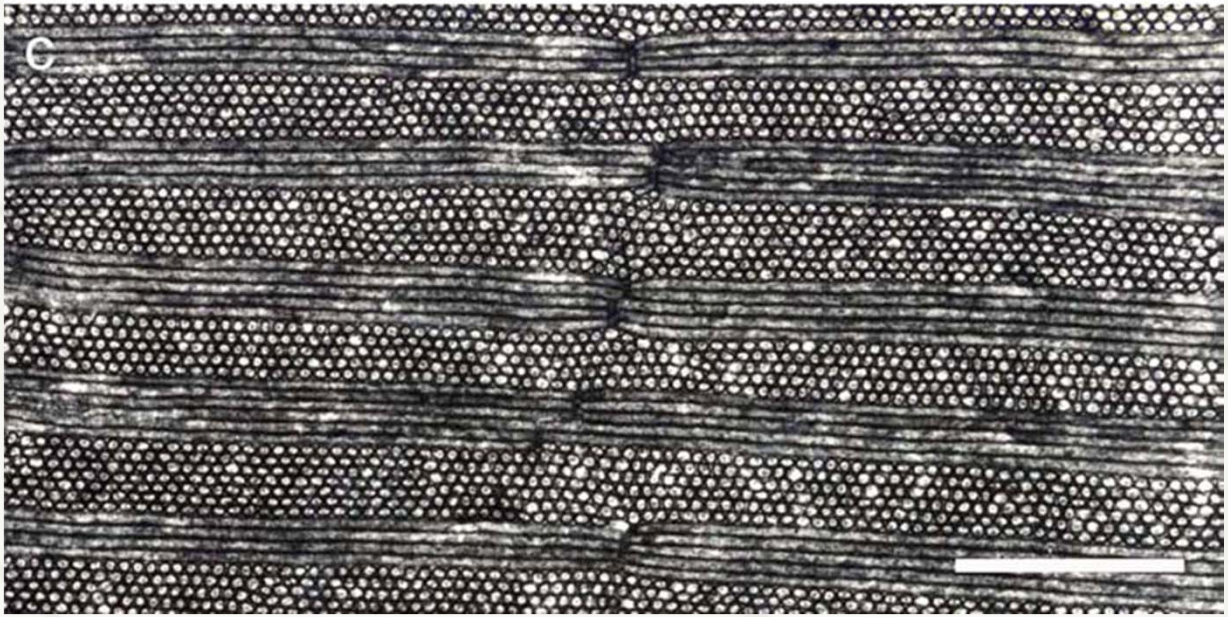
C

The
Crustacean
Wars
Clip Show

Bacillus anthracis

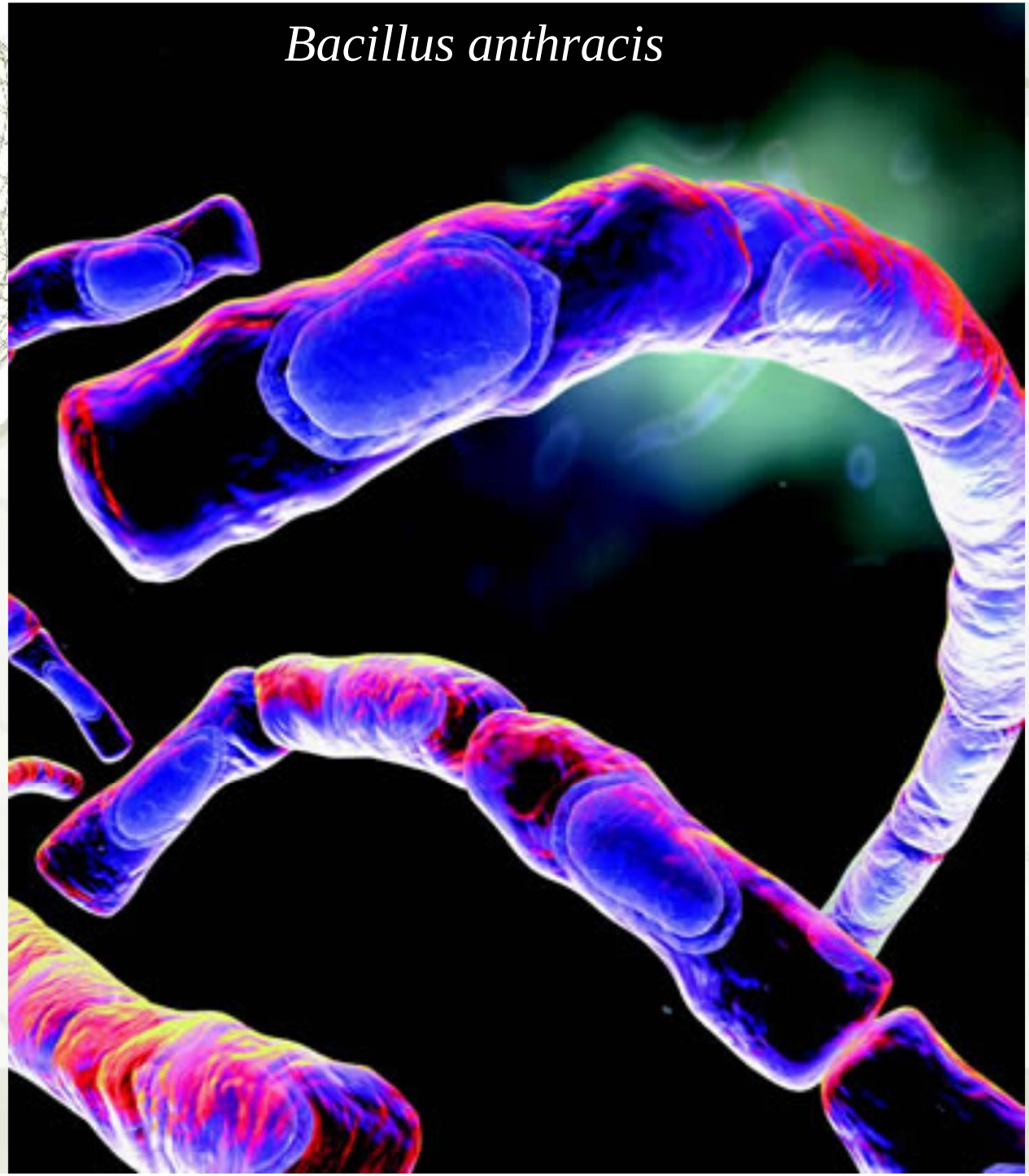

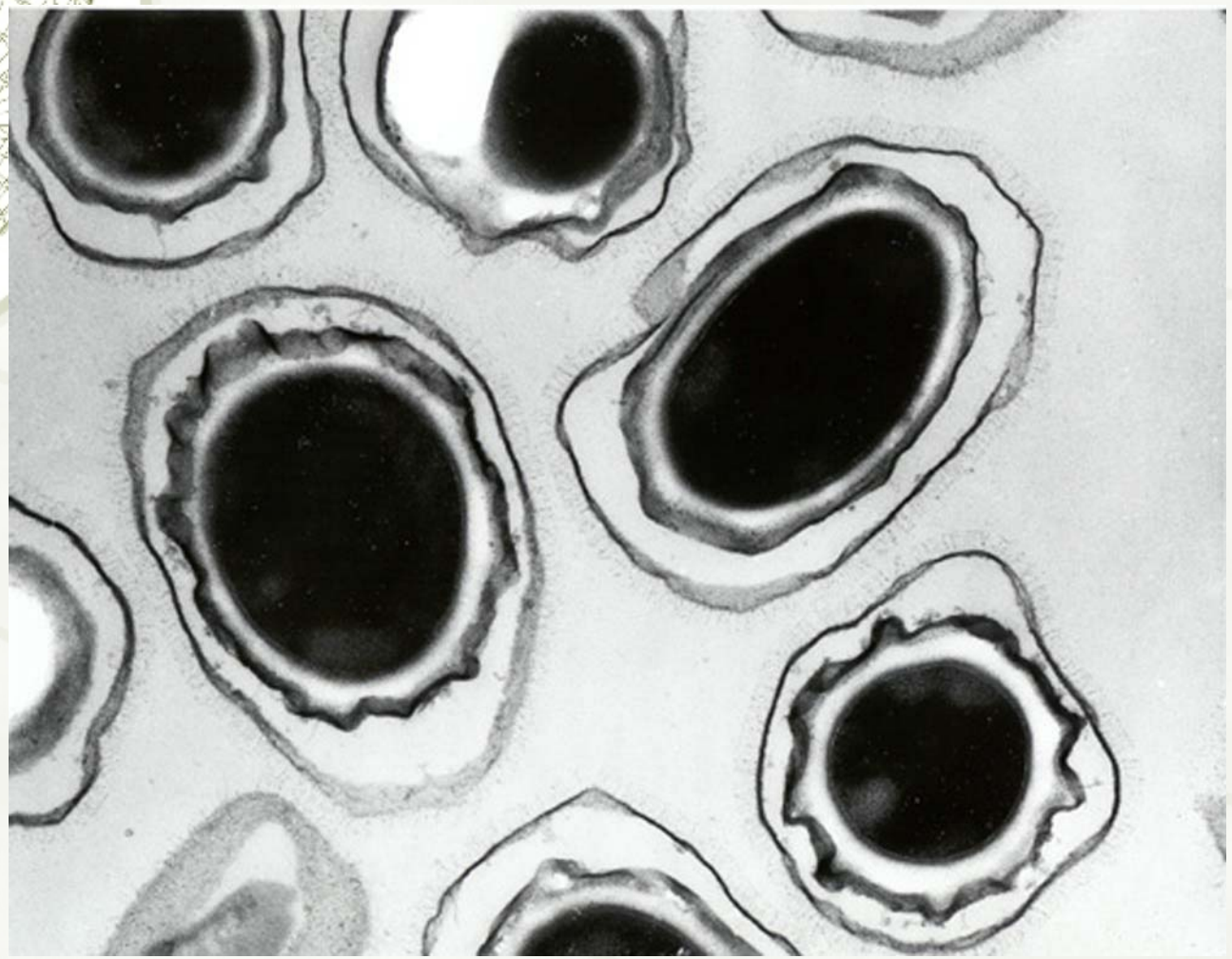

Particle Model-1: Spore

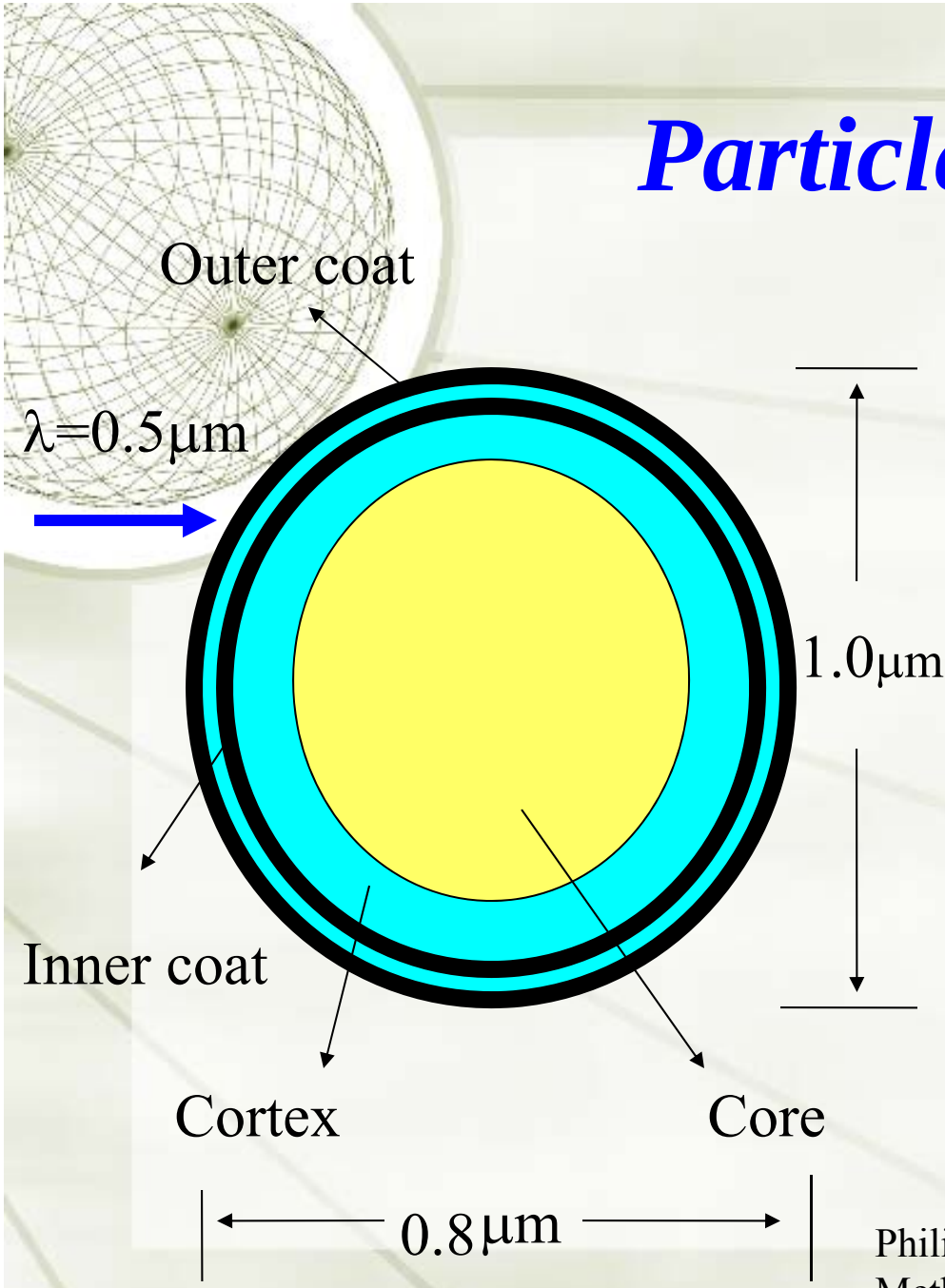

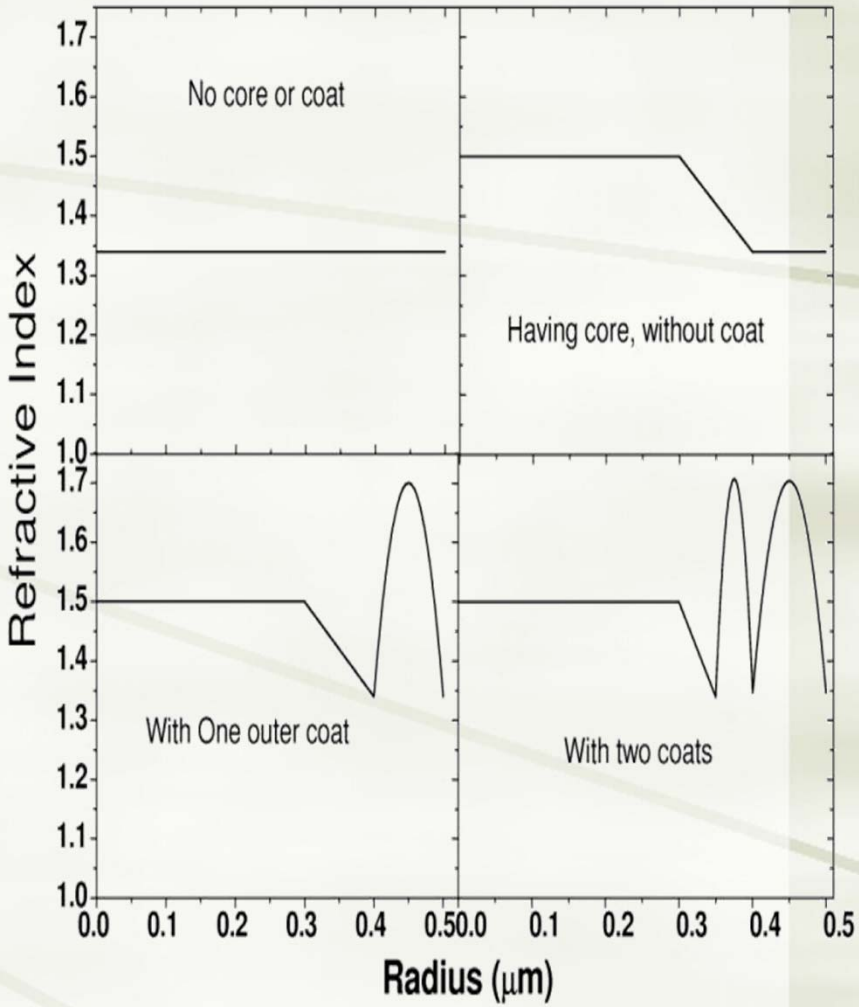

Philip J. Wyatt, "Differential Light Scattering: a Physical Method for Identifying Living Bacterial Cells", Applied Optics, Vol.7,No. 10,1879 (1968)

Simulation Models

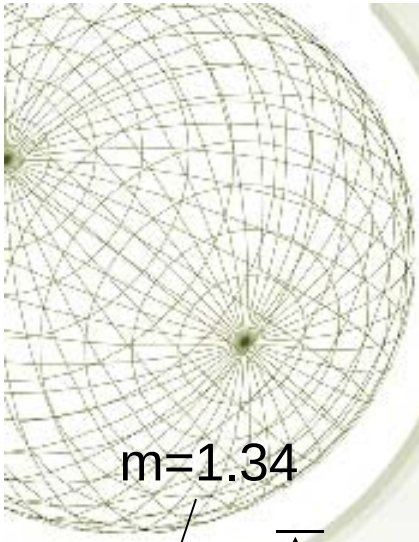

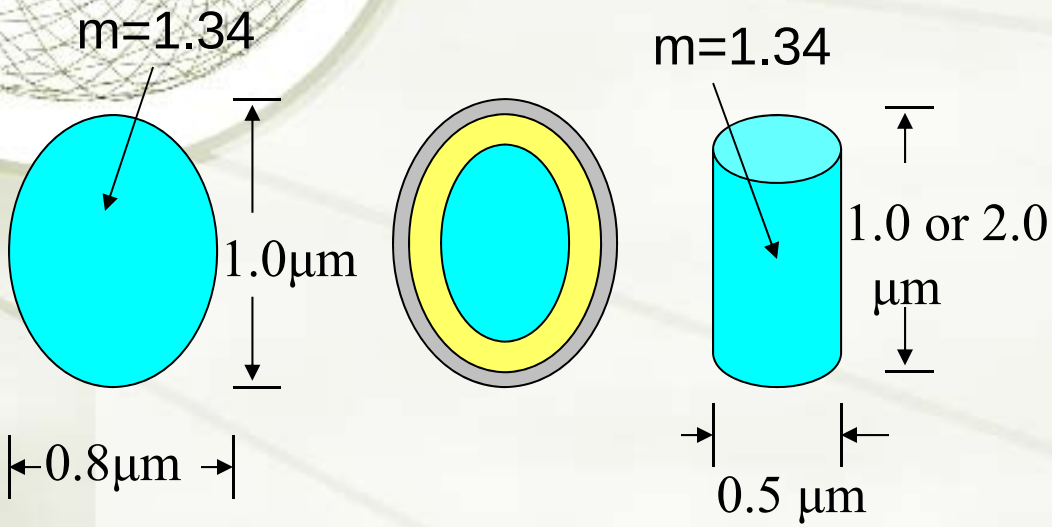

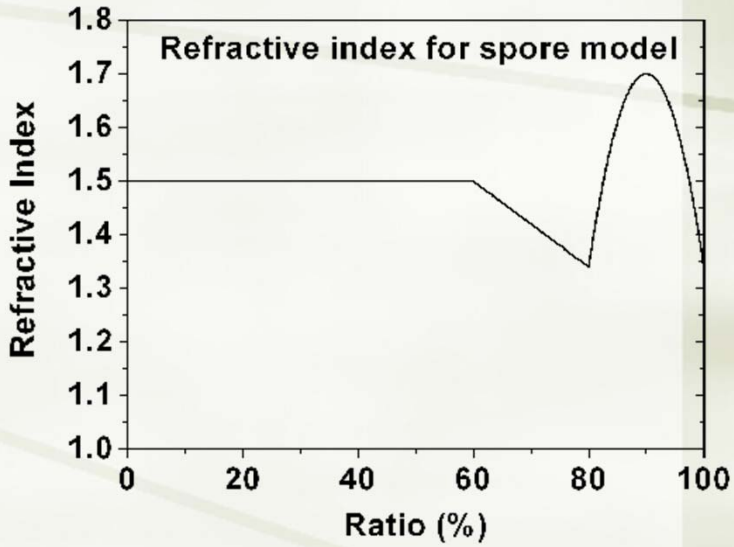

(a) (b) (c) (d)

Homogenous Spore Mueller Image

$\theta = 0^{o}$

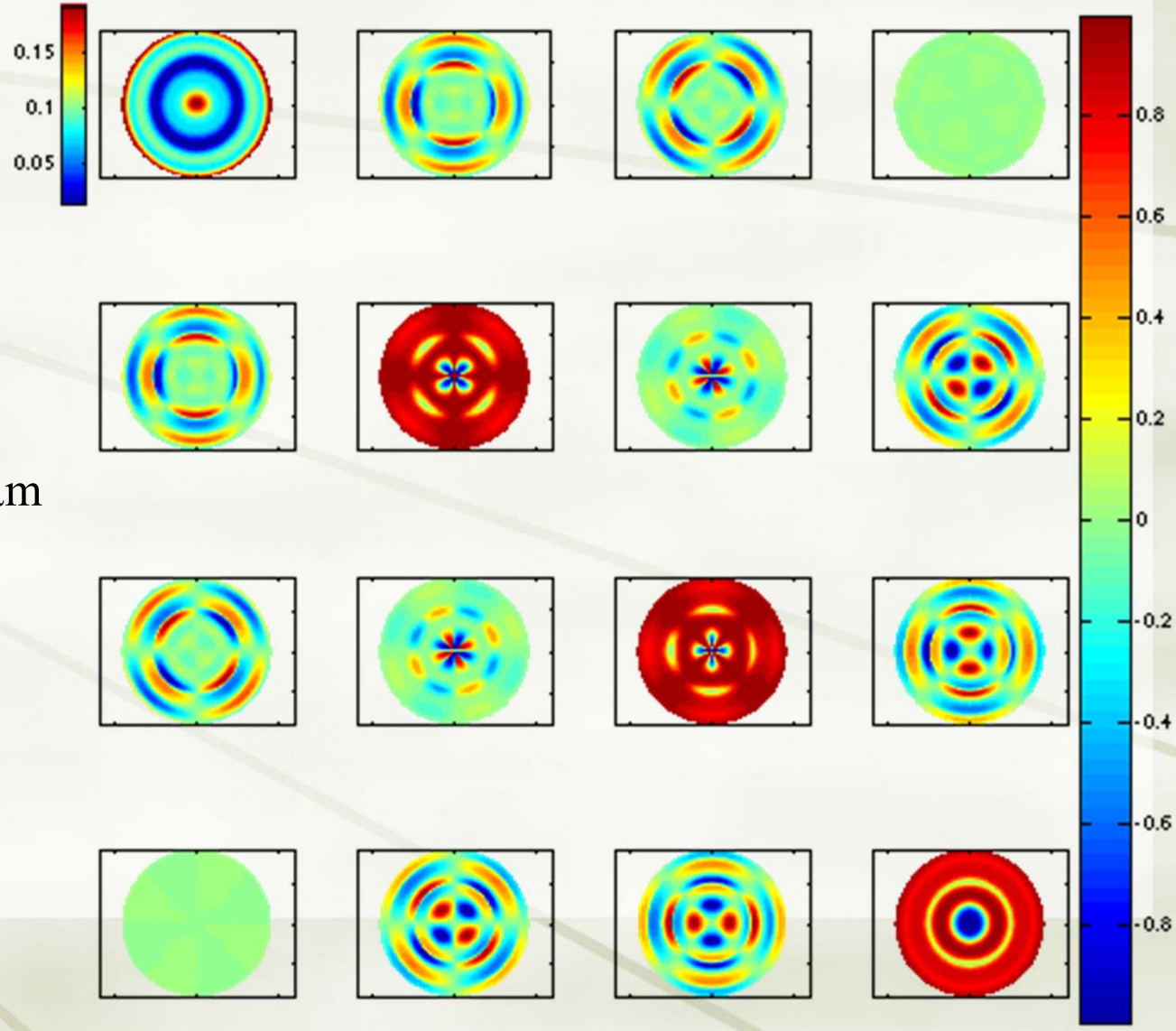

λ=0.5μm

m=1.34

1.0μm

0.8μm

Spore with Core Mueller Image

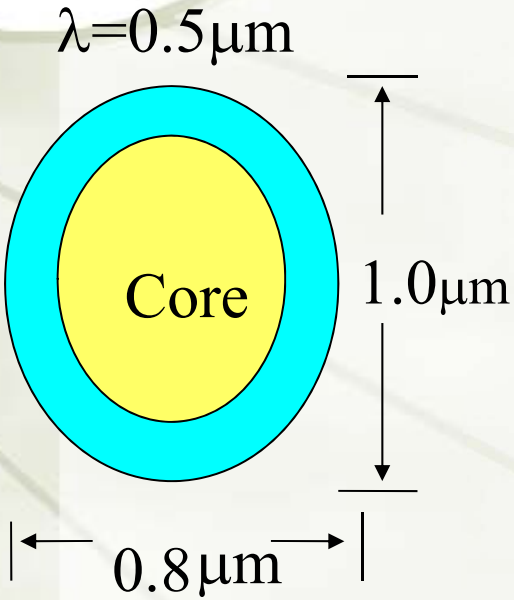

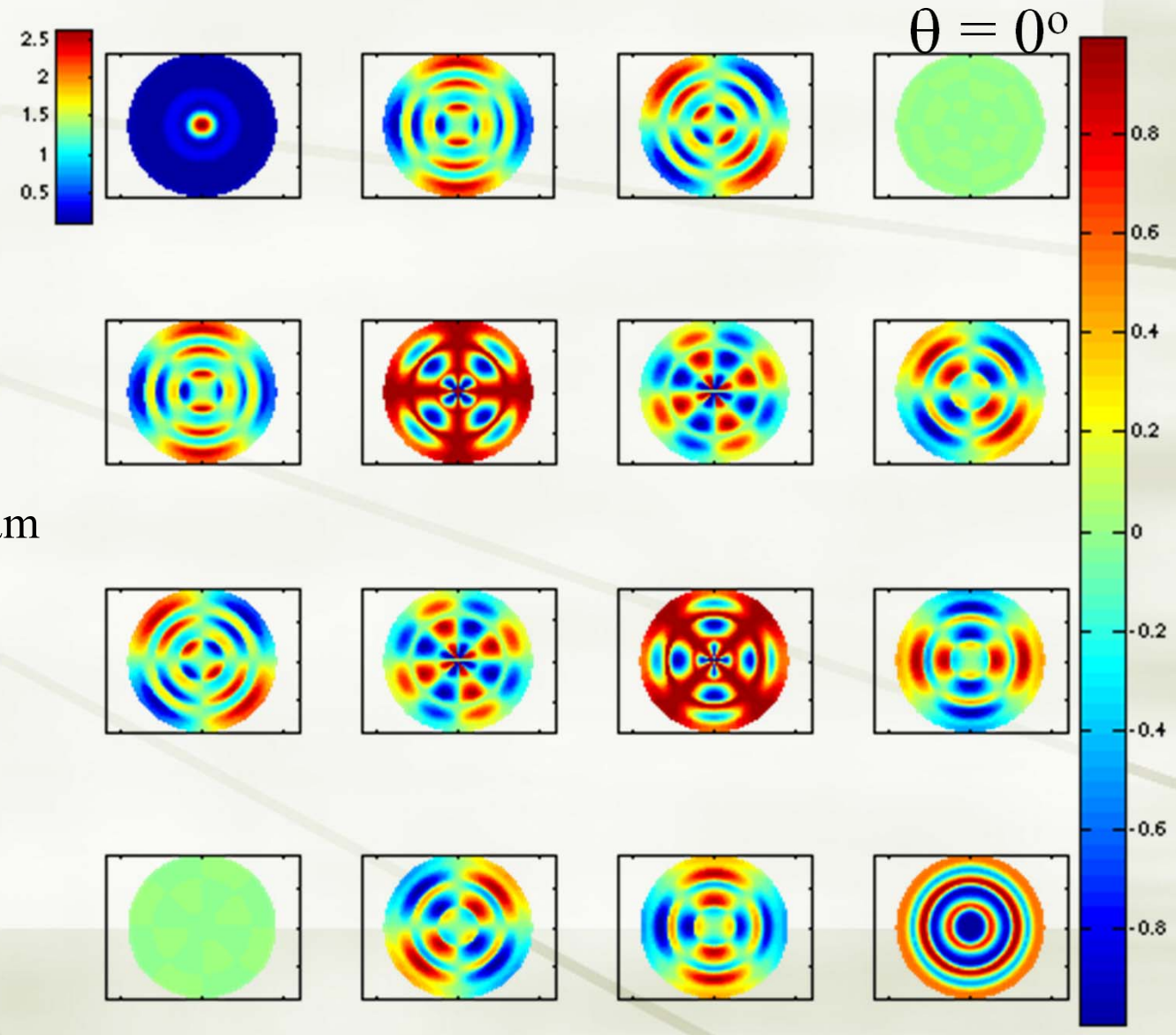

Homogenous Cylinder Mueller Image

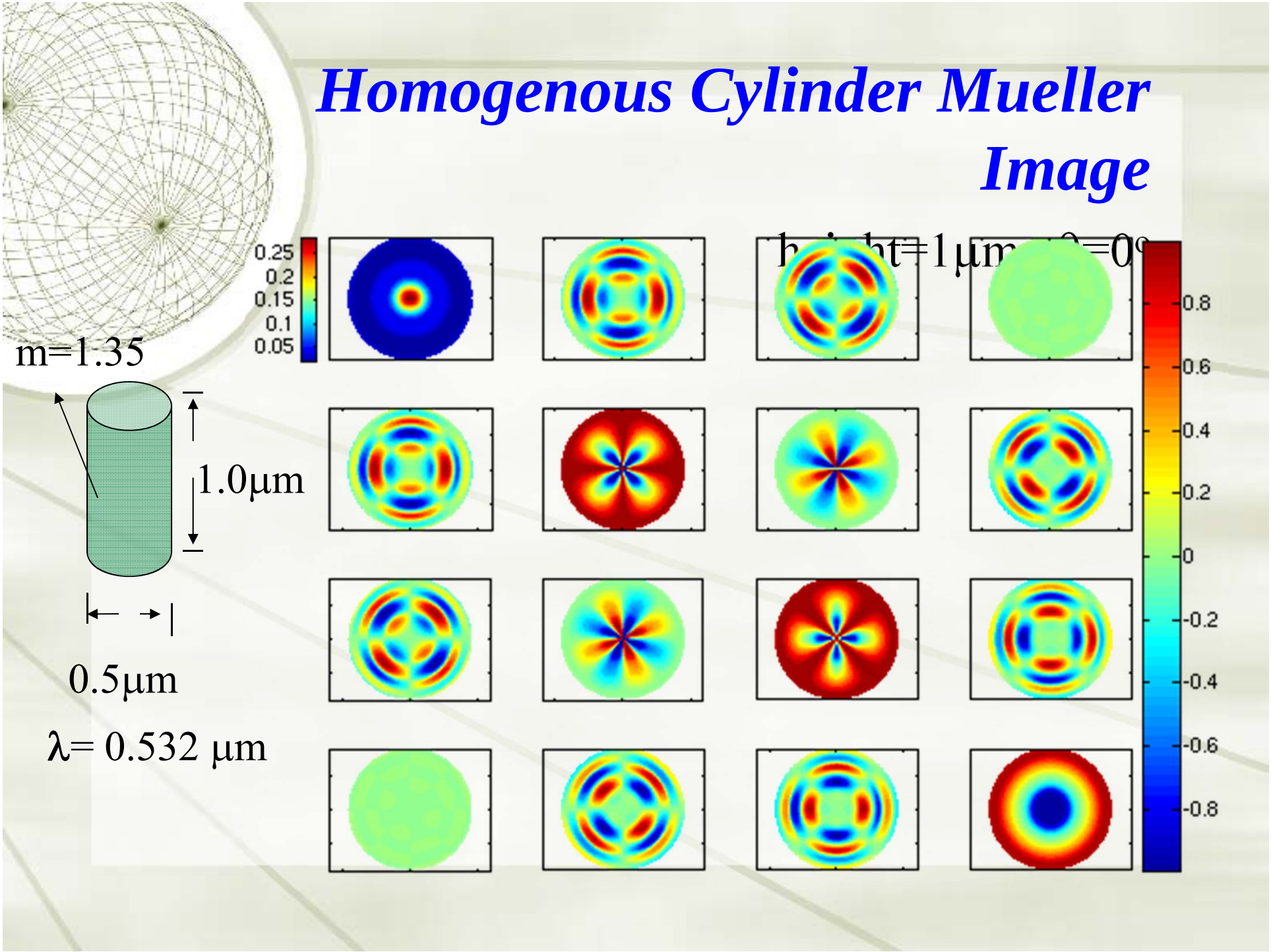

Mueller Image for Three Particles θ=90°

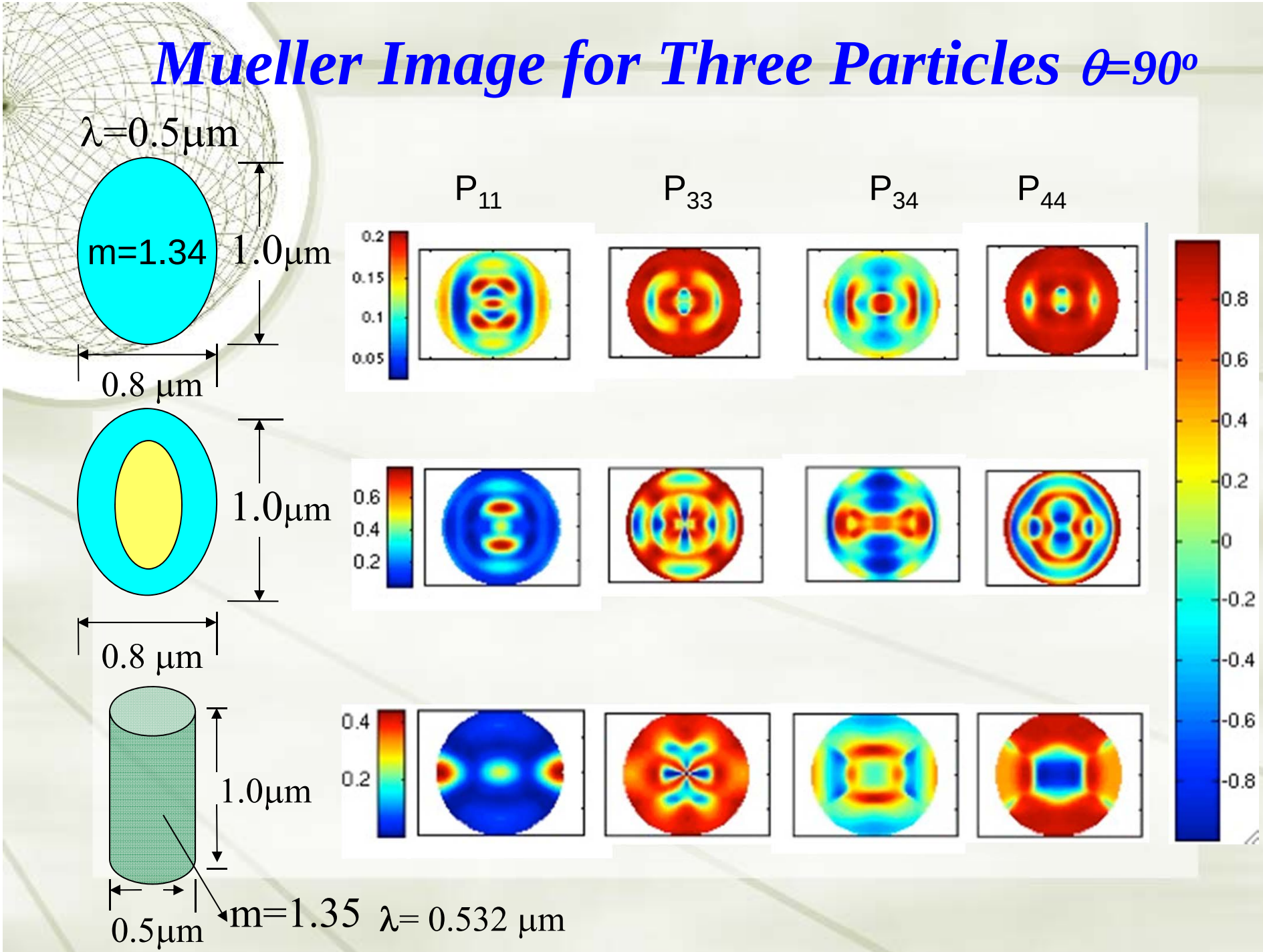

Polarized Light and Skin Cancer Detection

- Skin cancer, most common of all cancers (~50%)
- >1M cases of basal and squamous cell carcinomas in the US/year
- Melanomas account for 5% of all skin cancers
- If detected early, over 99% cure rate
- Visual inspection is only way to diagnose, but one-third are misdiagnosed
- Subsequent biopsy of the lesion
  - invasive, expensive, and time-consuming process
- There is a need for the development of accurate, non-invasive skin cancer detection or facilitated biopsy

Ref: American Cancer Society web site. http://www.cancer.org (updated on 05/06/2009)

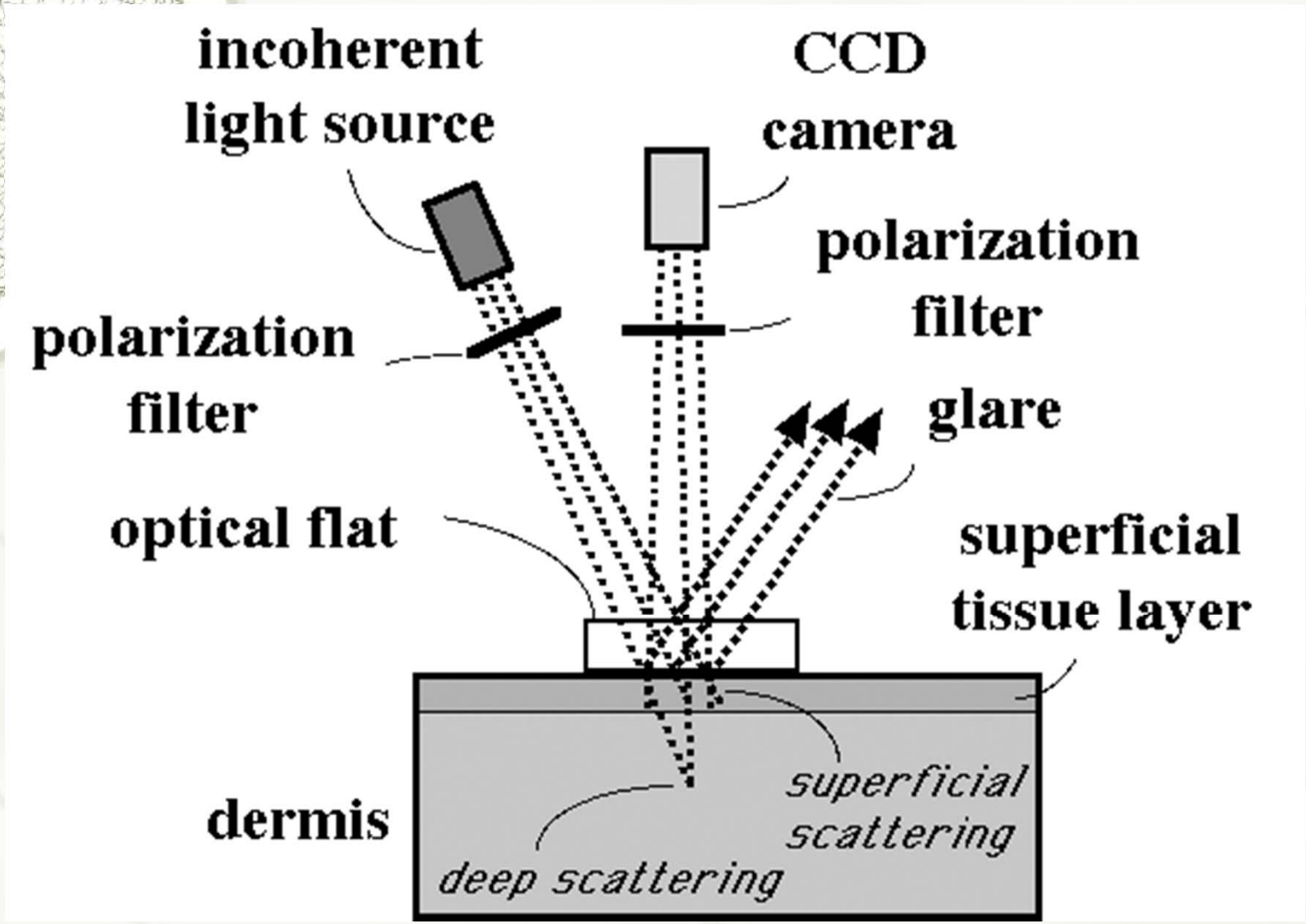
incoherent
light source
CCD
camera
polarization
filter
polarization
filter
glare
optical flat
superficial
tissue layer
dermis
superficial
scattering
deep scattering

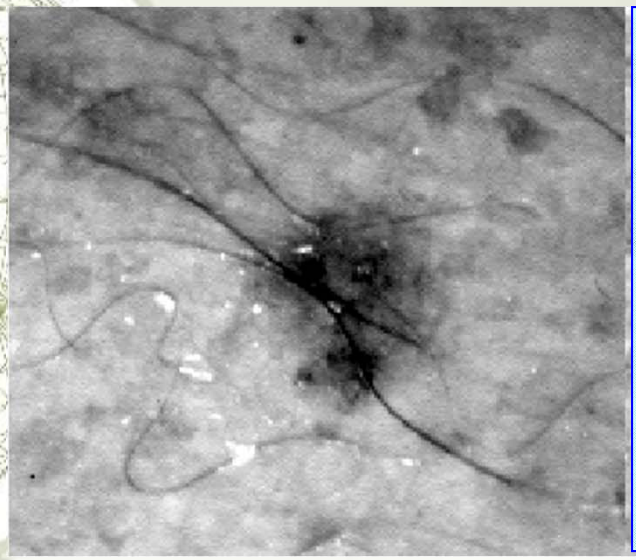

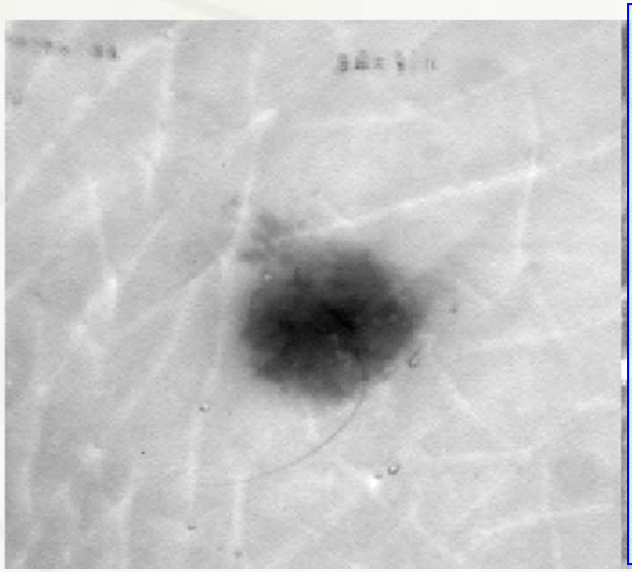

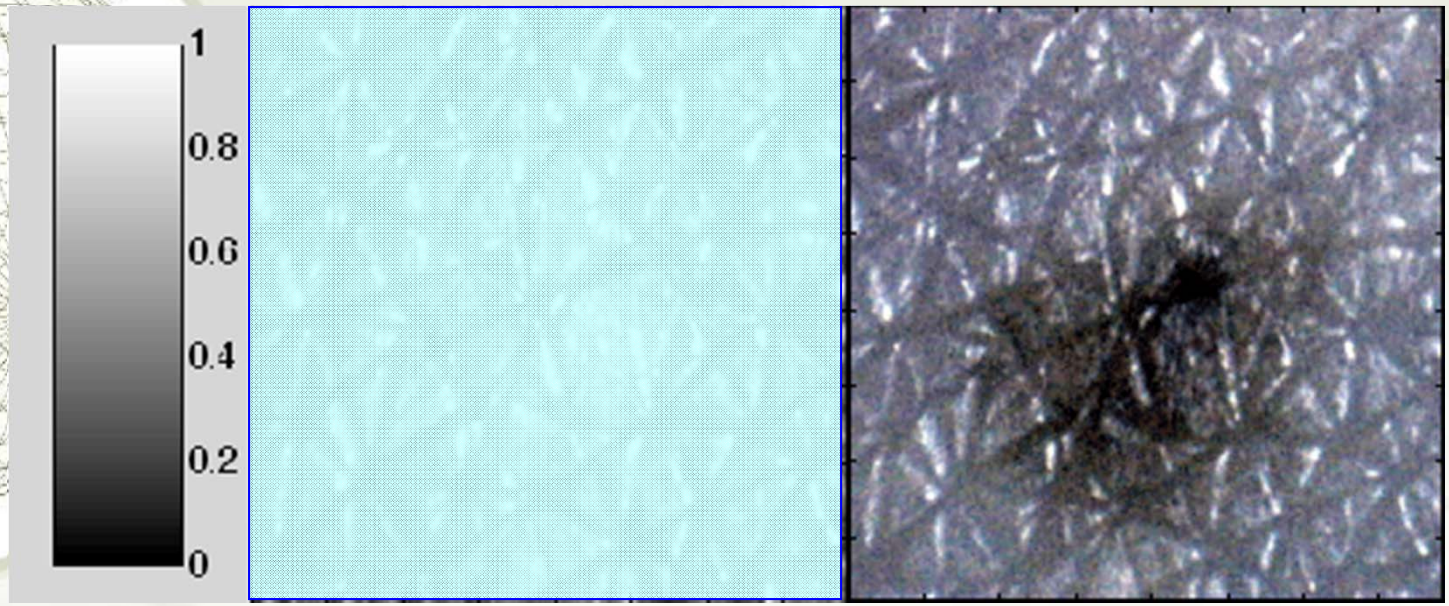

Image of a freckle; on the left we show the polarized image on the right the Horizontal image

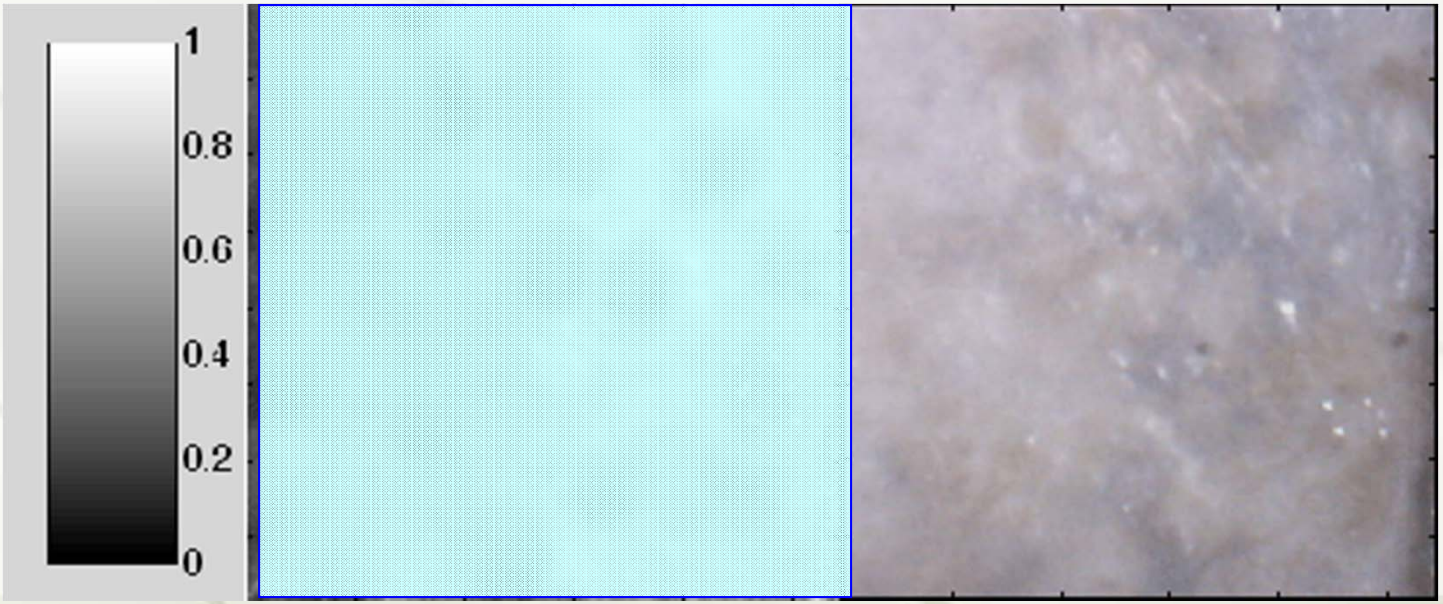

Image of a melanoma; on the left we show the polarized image on the right the Horizontal image

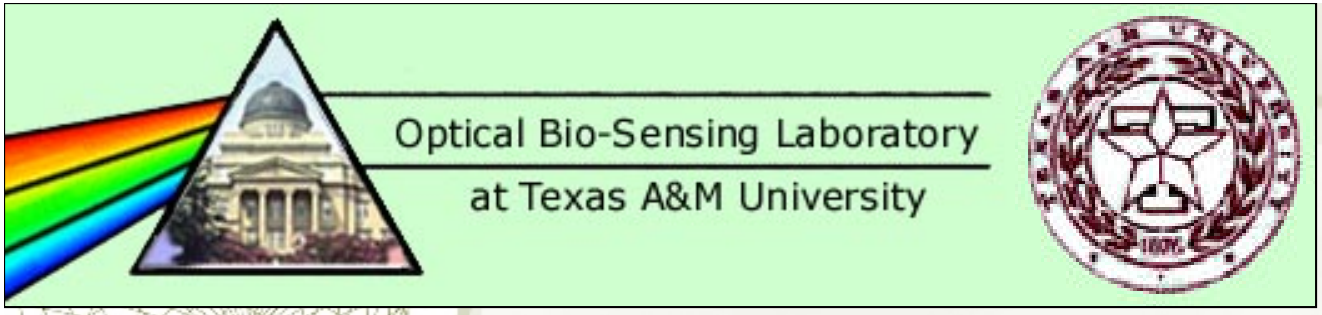

Interpretation Mueller matrix images based on polar decomposition and statistical discriminators to distinguish skin cancer

J.R. Chung[1], A.M. Baldwin[1], J.S. Baba[1],

C.H. Spiegelman[2], M.S. Amoss[3], and G.L. Coté[1]

[1]Department of Biomedical Engineering

[2]Department of Statistics

[3]Department of Veterinary Physiology & Pharmacology

Optical Bio-Sensing Laboratory
at Texas A&M University

Pig Skin – In Vivo

- Used Sinclair swine model
  - 85% incidence of Melanoma
- Imaged 3 types of tissue
  - Normal Skin
  - Benign mole
  - Cancerous Skin
- Three types of analysis
  - Mueller matrix
  - CART analysis
  - Polar Decomposition

Optical Bio-Sensing Laboratory
at Texas A&M University

Results: Polar Decomposition

Normal **Benign Mole** **Cancer**

Depolarization images

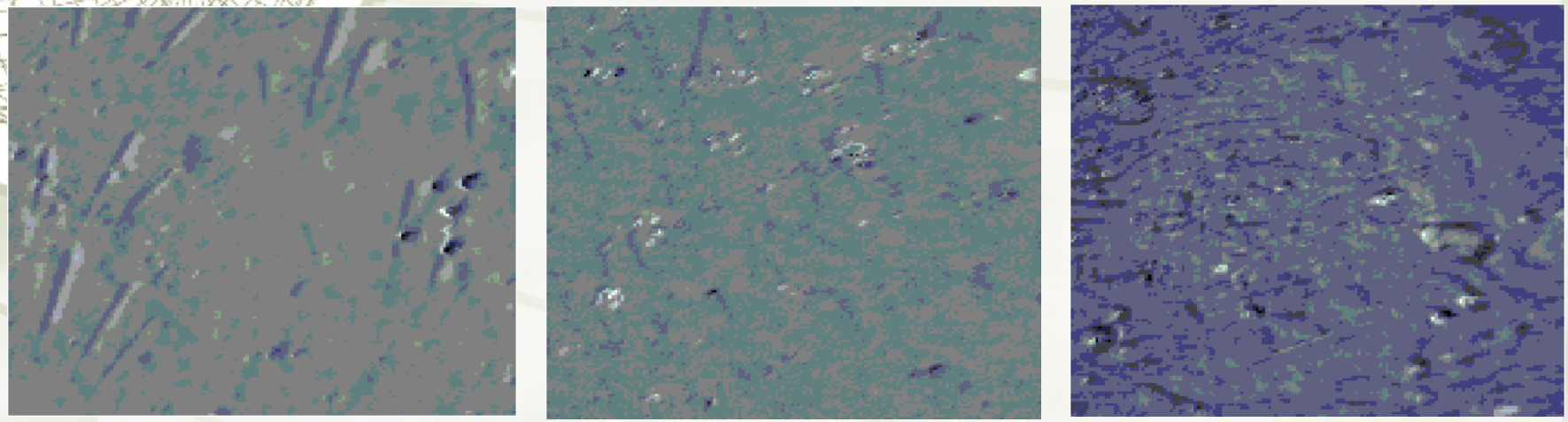

- Depolarization Index(DI): To discriminate between cancerous and normal tissue
  - DI = 0 (no depolarized)
  - DI = 1 (completely depolarized)
  - 0 < DI < 1(partially depolarized)
- The benign mole is indistinguishable from the normal tissue.
- The cancerous tissue depolarizes light less than the non-cancerous tissue.
- But, not visible the boundary of cancer lesions.

Optical Bio-Sensing Laboratory
at Texas A&M University

Results: Polar Decomposition

Normal **Benign Mole** **Cancer**

Diattenuation images

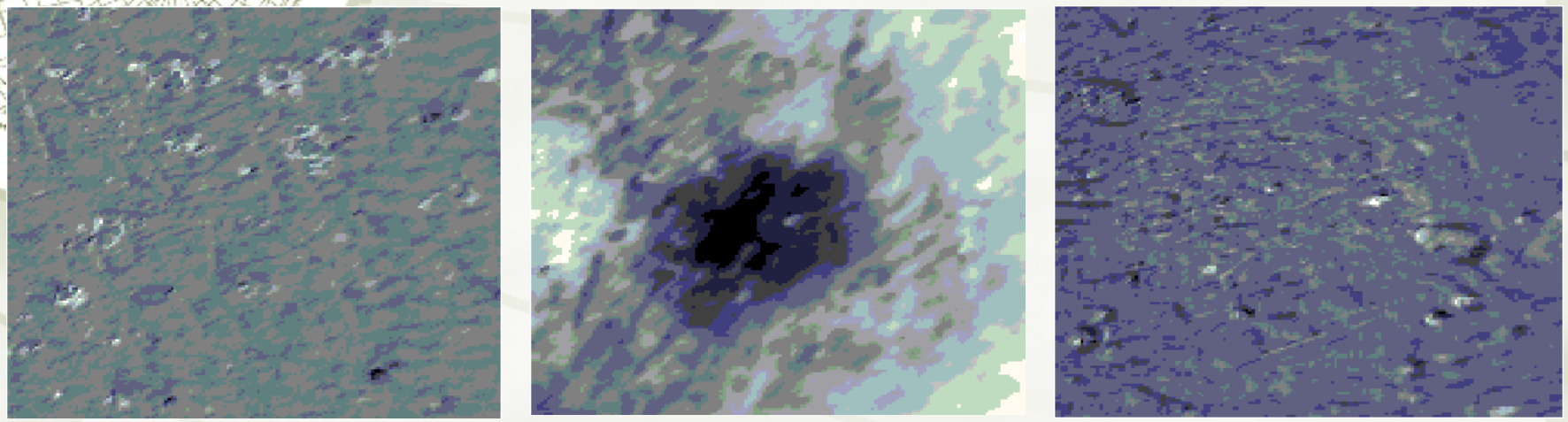

- The diattenuation and retardance images contain information about complex refractive index of the tissue
- The benign mole is distinguishable from the normal tissue
- But, not visible the boundary of cancer lesions.

Optical Bio-Sensing Laboratory
at Texas A&M University

Results: Polar Decomposition

Normal **Benign Mole** **Cancer**

Retardance images

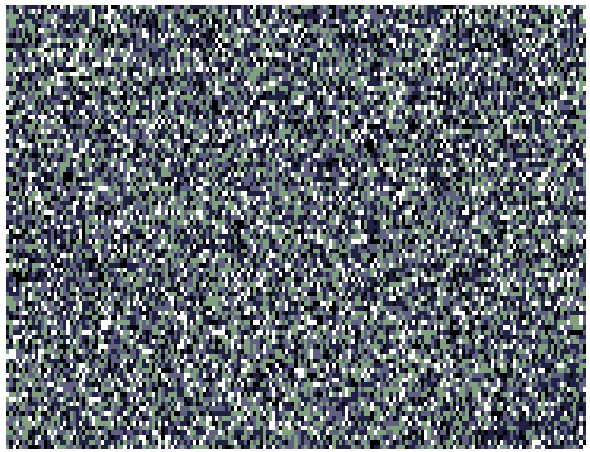
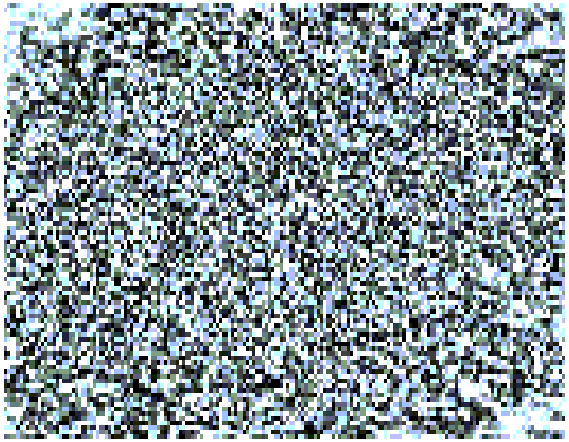
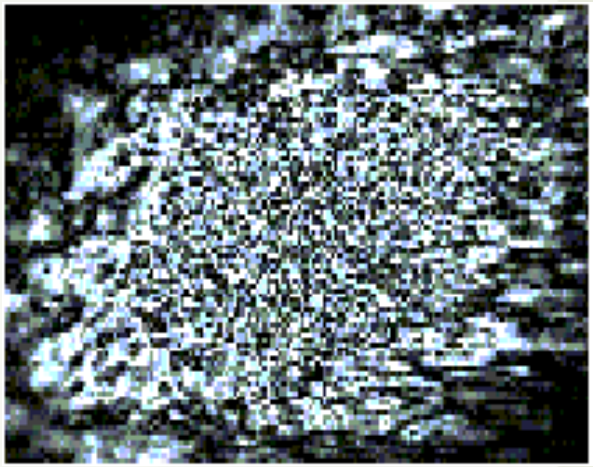

- No change for non-cancerous samples (normal, benign mole)
- The cancerous lesion is distinguishable from surrounding tissue.
- These retardance images are useful
  - for differentiating between samples
  - for boundary identification

Optical Bio-Sensing Laboratory
at Texas A&M University

Conclusion

- From Mueller matrix images, there is a noticeable difference between non-cancerous and cancerous tissue.
  - Underlying structure
- From Depolarization images, cancerous tissue depolarizes less than non-cancerous tissues.
- From Diattenuation images, the benign mole can be distinguished from the normal tissues.
- From Retardance images, not only differentiating between samples, but also for boundary identification.

Plankton as viewed by a squid

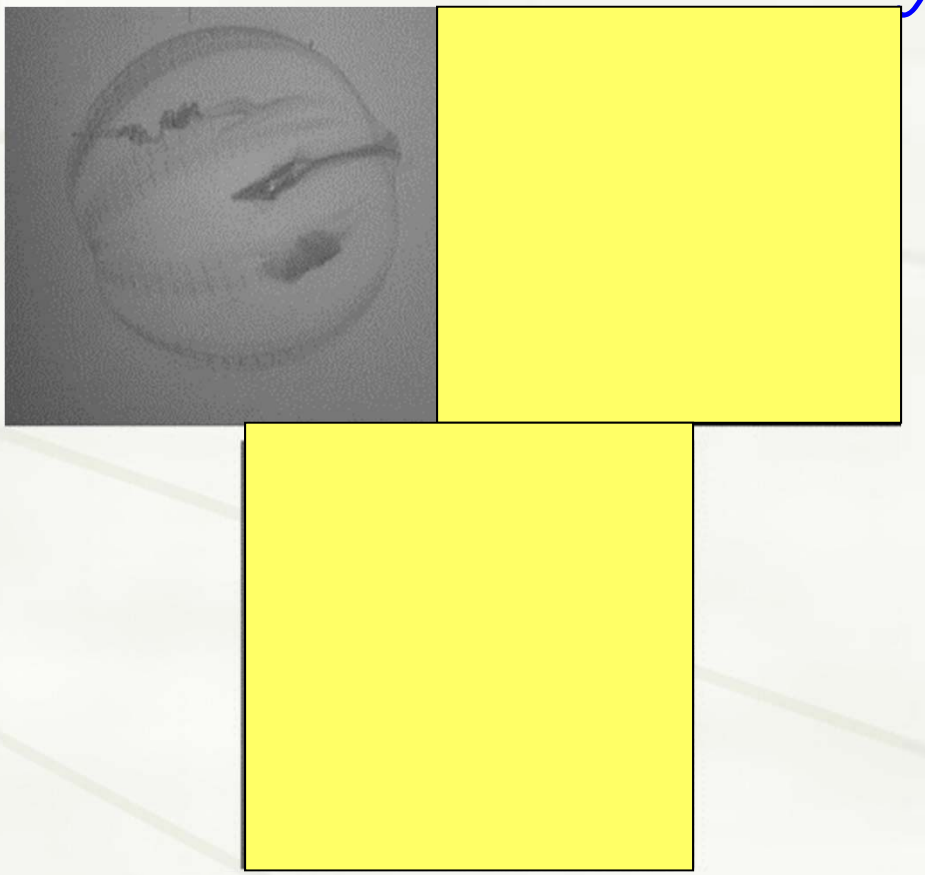

Planktonic animal as seen through "regular" vision

As seen when placed between two crossed linear polarizing filters

As seen by putting the two polarizers at 45° to each other

Roger T. Hanlon